AD_____
(Leave blank)

Award Number: W81XWH-10-1-0157

TITLE: Breast Cancer Tissue Bioreactor for Direct Interrogation and Observation of Response to Antitumor Therapies

PRINCIPAL INVESTIGATOR: Lisa McCawley

CONTRACTING ORGANIZATION:

Vanderbilt University Medical Center
Nashville, TN 37203

REPORT DATE: July 2012

TYPE OF REPORT: Annual

PREPARED FOR: U.S. Army Medical Research and Materiel Command
Fort Detrick, Maryland 21702-5012

DISTRIBUTION STATEMENT: (Check one)

× Approved for public release; distribution unlimited

□ Distribution limited to U.S. Government agencies only; report contains proprietary information

REPORT DOCUMENTATION PAGE

Form Approved
OMB No. 0704-0188

1. REPORT DATE	**2. REPORT TYPE**	**3. DATES COVERED**
July 2012	Annual	1 July 2011- 30 June 2012

4. TITLE AND SUBTITLE
Vanderbilt University Medical Center
Nashville, TN 37203

5a. CONTRACT NUMBER

5b. GRANT NUMBER
W81XWH-10-1-0157

5c. PROGRAM ELEMENT NUMBER

6. AUTHOR(S)
Lisa McCawley

E-Mail:

5d. PROJECT NUMBER

5e. TASK NUMBER

5f. WORK UNIT NUMBER

7. PERFORMING ORGANIZATION NAME(S) AND ADDRESS(ES)
Vanderbilt University Medical Center
Nashville, TN 37203

8. PERFORMING ORGANIZATION REPORT NUMBER

9. SPONSORING / MONITORING AGENCY NAME(S) AND ADDRESS(ES)
U.S. Army Medical Research and Materiel Command
Fort Detrick, Maryland 21702-5012

10. SPONSOR/MONITOR'S ACRONYM(S)

11. SPONSOR/MONITOR'S REPORT NUMBER(S)

12. DISTRIBUTION / AVAILABILITY STATEMENT
Approved for Public Release; Distribution Unlimited

13. SUPPLEMENTARY NOTES

14. ABSTRACT

Tumor tissue is made up of tumor cells and other surrounding cell types in its microenvironment. This diseased tissue frequently exists in specialized tumor microenvironment such as being less oxygenated and more acidic than healthy tissue. These states profoundly impact anti-tumor drug efficacy. For disease diagnosis, a tumor is frequently biopsied. We believe that if we can maintain a biopsied portion of the tumor tissue in a similar tumor microenvironment, that we can preserve the exact same tumor cellular functions ex vivo. The objective of this project is to develop biomicroelectromechanical systems (BioMEMs), the Breast Cancer Tissue BioReactor that will support the combination of the 3-D culture methodology with control over microenvironmental oxygen and matrix stiffness to better approximate the in vivo tumor microenvironment ex vivo. This setting then would allow testing of anti-tumor drug responsiveness using a patient's own tumor tissue targeted with anti-drug therapeutics. We will test our BCTB using mouse models of breast cancer.

15. SUBJECT TERMS- Bioreactor, tumor microenvironment, breast cancer, microfluidics

16. SECURITY CLASSIFICATION OF:			**17. LIMITATION OF ABSTRACT**	**18. NUMBER OF PAGES**	**19a. NAME OF RESPONSIBLE PERSON**
					USAMRMC
a. REPORT	**b. ABSTRACT**	**c. THIS PAGE**			**19b. TELEPHONE NUMBER** *(include area code)*
U	U	U	UU		

Table of Contents

INTRODUCTION:

Tumor tissue is made up of tumor cells and other surrounding cell types within its microenvironment(1-4). Furthermore, this diseased tissue frequently exists in a less oxygenated (termed "hypoxic") environment than does healthy tissue(2;3;5;6). This unique state selects for cell populations that thrive in this harsh climate. All of these states profoundly impact anti-tumor drug efficacy(5;7-10). Frequently, tumor biopsies are used to assess the state and progression of the disease. We believe that if we can maintain a biopsied portion of the tumor tissue in a similar tumor microenvironment, that we can preserve the exact same tumor cellular functions ex vivo. This setting then would allow testing of anti-tumor drug responsiveness using a patients own tumor tissue targeted with anti-drug therapeutics. The objective of this project is to develop biomicroelectromechanical systems (BioMEMs) that will support the combination of the 3-D culture methodology with control over microenvironmental oxygen and matrix stiffness to better approximate the *in vivo* tumor microenvironment *ex vivo*. We are fabricating the proposed BioMEMS devices and the sensor arrays used to substantiate the base oxygen and pH gradients using soft lithography and thin film deposition techniques. Matrix tension in being altered by using defined ECM compositions to generate patterns of matrix stiffness. These devices and capabilities are currently being validated using traditional normal and tumorigenic mammary epithelial cell culture systems grown under 3D cell culture conditions that allow for mammosphere or glandular mammary acinar development. Drug delivery into the device has been validated using a Protease inhibitor compound that can inhibit mammosphere formation within the BCTB. Xenografts generated in mice will be used for biopsy samples to validate the maintenance of the *in vivo* tumor cellular functions *ex vivo* in the Breast Cancer Tissue BioReactor. Once these base line conditions are established, we will correlate the drug response of the tumor biopsy challenged within the Breast Cancer Tissue BioReactor with the corresponding outcome *in vivo* against xenograft models of the same.

BODY:

Breast Cancer Tissue Bioreactor for Direct Interrogation and Observation of Response to Anti-Tumor Therapies.

Our work this year focused on 3 key areas: 1) validating drug delivery in the system including a dose dependent response of docetaxel into the system. We also worked on a manuscript and currently have a paper published of this current base design including drug delivery!!!; 2) continued development of the Breast Cancer Thick-tissue Bioreactor to include controlled oxygen and in particular working out toxicities of the oxygen thin films and 3) continued development of the Breast Cancer Thick-tissue Bioreactor to include controlled pH environments which necessitated exploring additional pH sensors. In combining oxygen, pH and matrix stiffness, our design features delivery of gas (i.e., oxygen and nitrogen) through PDMS. Thus, determining the parameters controlling diffusion of gas through PDMS with various treatments (i.e., surface treatments, increasing cross-linking of PDMS) was essential for the design features. Regarding item #3, we had an unanticipated hurdle this year. Last year, as we developed the thin films and moved to apply this tool with long-term cell culture, we began to sterilize with our standard techniques and had a difficulty with maintaining sample integrity. We tested a variety of conditions and have a good sterilization protocol currently. However, there were toxicities

noted in the cells when we began culturing for long-term within the reactor that were unanticipated.. This is described in detail below.

Task 1: To Develop the Breast Cancer Tissue Bioreactor (BCTB) and functionalize with controlled matrix rigidity in the surrounding microenvironment.

A) Develop and fabricate high throughput Breast Cancer Tissue Bioreactor (BCTB) disposable cartridges.

We continued to fabricate Breast Cancer Tissue Bioreactors (BCTB) as we described last year. BCTBs were fabricated in PDMS using standard soft lithography and replica molding techniques. The device consists of two parts: a 1 mm thick PDMS membrane that contains four 3 mm in diameter Cell/Biopsy growth chambers (separated by 5.85 mm) and a top 4 mm thick PDMS piece that contains the microfluidic supply networks for each chamber (Figure 1A and B). The membrane is bonded to a 2" x 3", 1 mm thick glass slide to provide structural support and to allow cell imaging through an inverted microscope. Growth chambers are in direct contact with supply networks or are separated from microfluidic supply channels by a polycarbonate filter (Osmonics, Inc) with 0.4 micrometer pores, that maintains diffusional exchange of nutrients and waste products and prevents leakage of ECM into the microfluidic channels. The supply network for each of the cell growth chambers consists of 8 microfluidic channels 100 µm wide x 100 µm tall with 100 µm walls connected together to a larger 800 µm wide input / output regions of the network (Figure 1A and B). The entire reactor is clamped together under sterile conditions in a custom built polycarbonate and stainless steel clamp that allows for easy alignment of the reactor components, provides structural stability to the assembly, and evenly distributes holding pressure across the PDMS surfaces (Figure 1C and D). All 4 individual reactors in a single BCTB cartridge were gravity fed from a modified 14 mL tube with a loose fitting cap (i.e. a "snap cap tube") mounted in a custom built holder. The output of the feeding tube was directly connected to a 50 µm tall microfluidic manifold splitting the input flow

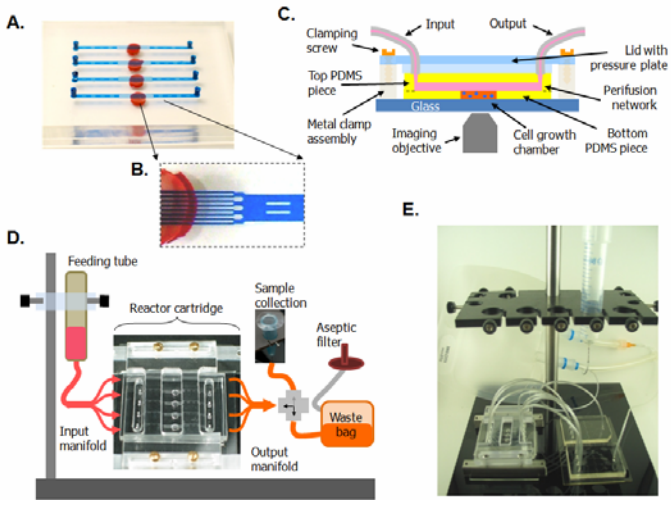

Figure 1. Design of the Thick Tissue Bioreactor (TTB). A) A photograph of the TTB filled with blue and red dyes indicating microfluidic supply network (blue) and the cell culture chambers (red) beneath the perifusion channels; B) A close view of the binary flow divider with ceiling support pillars and a cell culture chamber; C) Block-diagram of the typical layout for the clamped TTB indicating major components; D) A photograph of the clamped TTB cartridge with a schematic diagram illustrating the set-up for long-term culture; E) A photograph of the fully assembled TTB prototype with the gravity-driven feeding system, passively regulated flow through the input/output manifold, and a Labtainer™ from HyClone as a waste containment system. (11). Also see appendix.

into 4 even streams for each of the reactor within the cartridge. A second output manifold (on the waste side of the reactor) was used to passively regulate the flow rate as described in detail below; to recombine the outflow from 4 reactors; and, to direct it into a waste collection ("Labtainer" ™ from HyClone) or sample extraction systems (Figure 1D and E). The fluid levels in the feeding tube were always held at 15 cm above the surface. All tubing was 0.020" ID, 0.060" OD Saint-Gobain* Tygon* microbore tubing (Part # AAQ04103) from Fisher Scientific. In order to achieve targeted media exchange rates within the BCTB, we used differentially sized manifolds. Each individual channel in the input manifold was 100 μm wide and 50 μm tall. Our target flow rate of 700 nL/min (1 mL/day) is achieved with the output manifold height being 20 μm (maintaining channel width of 100 μm).

B) Establish BCTB with varying matrix stiffness . We will test the following methodologies in order:

NOTE: As we moved this year to doing side by side comparisons of multiple conditions together, the BME and pH differences were done jointly and are reported together below in Section 2B.

Task 2. To Develop Breast Cancer Tissue Bioreactor (BCTB) with controlled oxygen and pH in the surrounding microenvironment.

A) Adapt BCTB to include control of normoxic to hypoxic conditions within same BCTB cartridge. (M 1-14)

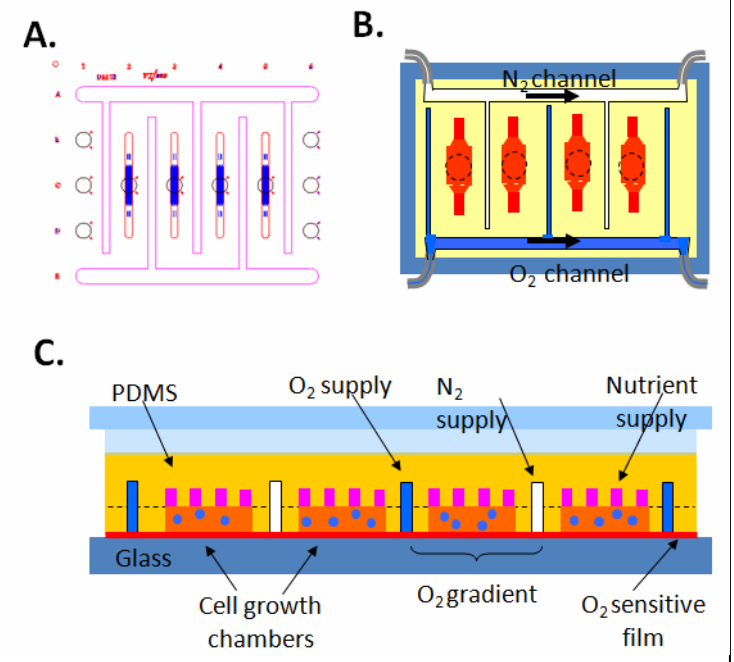

Figure 2. <u>Oxygen Gradient Formation</u>. A) Multilayer photolithographic masks for fabrication of modified BCTB with oxygen delivery network. BCTB with individually addressable gas channels allowing capability of maintaining each cell-culture chamber at distinct oxygen concentrations. Black circles illustrate cell-culture chambers, pink – gas delivery channels (oxygen sources and sinks), red and blue – nutrient delivery microfluidic channels. B,C) A scheme for O_2 delivery inside BCTB. Source and sink channels contain proper mixture of O_2 and N_2 to achieve target (normoxic / hypoxic) conditions.

i) Specific O_2 concentration will be established for each of the biopsy / cell chambers within the same BCTB cartridge, where each of compartment will experience a similar O_2 concentration (i.e. , normoxic or hypoxic).

We have designed several variations of the Breast Cancer tissue bioreactor cartridge with oxygen supply and drain channels to establish particular normoxic or hypoxic conditions. One design features single channels for both oxygen supply and sink with interdigitated blind extensions that provide a fixed oxygen concentration for all of the cell culture chambers within the BCTB cartridge shown in Figure 4. This is the format for providing defined oxygen concentrations within the BCTB that we are evaluating.

ii) Optimize 2-dimensional detection and quantification of O2 based on O2 sensitive thin film.

Oxygen sensitive compound Platinum(II)-tetrakis(pentaflourophenyl)porphyrin (Pt-TPFP) immobilized within a thin (~1.5 μm thick) polystyrene matrix spun on top of a standard microscope glass slide is as an oxygen sensor(12;13). It was found that adhesion of such film to a microscope slide in the wet environment of cell culture was drastically improved if the glass slides were pre-coated with 1% solution of polyvinyl alcohol (PVA) before depositing a 10% w:v solution of polystyrene in toluene containing Pt-TPFP in 1:100 w:w to PS. The thickness of the adhesion promoting PVA layer was several nanometers and did not significantly affected the overall film thickness. As oxygen diffuses through the 1.5 μm thick PS film it interacted with the Pt-TPFP immobilized within the film quenching its fluorescence. Fluorescence images are taken with Zeiss microscope Axiovers 25 equipped with QColor 5 cooled ccd camera, and Tx Red fluorescence filter set. Before each experiment film performance is calibrated with 0%, 21%, and 100% oxygen and Stern-Volmer relationship was used to determine quenching constant Ksv. As we continue to fabricate oxygen sensitive films, we continue to monitor the quenching constant for batch to batch variation.

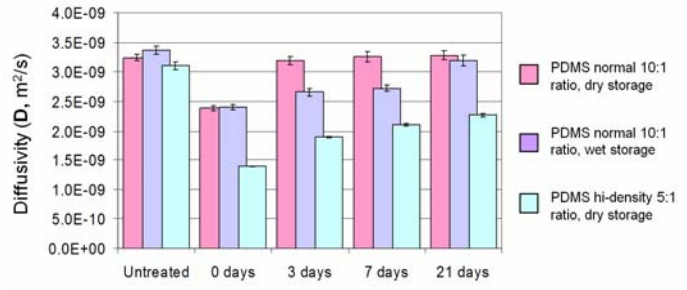

Figure 3. Experimentally determined oxygen diffusivity through 1 mm thick PDMS membranes as a function of surface properties and storage conditions. Note: 1) normal and high density PDMS have almost identical O_2 diffusivities in native state; 2) initial plasma treatment significantly decreases O_2 diffusivity, in some cases by more that 50%; 3) original diffusivity values are fully restored in 3 days for normal PDMS stored in air, while hi-density PDMS does not recover in 3 weeks under the same storage conditions; storage under water (normal operating conditions for a bioreactor) delays recovery by 3 weeks. Error bars represent the 95% confidence interval based on 3 independent measurements with 3 different membranes.

As we reported last year, during our preliminary experiments, we noted that the time it took for oxygen to be delivered to the cell culture chamber varied significantly with age of our BCTB cartridges. In order to estimate time evolution of oxygen gradients, the effect of PDMS treatments with oxygen plasma and consecutive aging of the surface, we fabricated a series of PDMS membranes, subjected them to various treatments and determined diffusion coefficients of oxygen across them. In order to determine oxygen diffusion coefficients, the treated PDMS membranes were placed on top of the Pt-TPFP oxygen sensitive film and clamped with a Plexiglas lid containing a gas delivery channel. Using the Stern-Volmer relationship and Fick's Law of diffusion, the diffusivity of oxygen in PDMS was measured for the untreated, freshly treated, and aged membranes for normal (10:1) and more dense (5:1) PDMS formulations. We have continued our testing until we could achieve significance to validate our finding. Furthermore, last year we tested various sterilization

methods and compatibility of the film sensor with other standard tissue culture reagents (for example, ECM and phenol red in media). These findings are in preparation for publication.

Based upon these findings, we moved to begin using our thin films to analyze controlled oxygen delivery into our BCTB. In our initial biocompatibility studies, we observed that MCF10A and their variants grew normally for short-term cultures on top of PS film containing Pt-TFPP when cultured open-faced inside cell culture chambers placed in standard Petri dish. Based upon this, we moved to long-term culture within the BCTB and discovered that the mammospheres seized growing and began to die off under extended (over 48 hour) culture conditions. Following a week of culture, we lost all mammosphere cultures inside the BCTB that contained oxygen sensitive thin-films. Using standard oxygen delivery, we observed mammosphere formation in cultures both in the presence and absence of the PS film containing Pt-TFPP and only those cultures on top of the oxygen sensitive film were affected. Dr. Markov and collaborators had previously used similar thin films to analyze oxygen level effects on amoeba cultures under aerobic and aneorobic conditions mimicking growth in soil. The amoeba cultures were unaffected by the presence of the PS film containing Pt-TFPP. Thus, we had thought that biocompatibility of PS film containing Pt-TFPP would not be an issue. It appears to be something evident only with longer culture times. We spent significant amount of time testing and developing various treatments to the film sensor. In the end, what we have found was that allowing films to rest after fabrication for at least a week and soaking them for at least 24 hours in either water or 1x PBS prior to using in conjunction with the BCTB eliminates previously observed cytotoxicity. We entertained one possibility that there were micro-scratches to the surface of the oxygen sensitive film that allowed penetration of trace inorganic reagents used in the making of the thin film into the culture system. However, physically scratching the surface of the oxygen sensitive thin films did nothing to alter the susceptibility to toxicity. We speculate that there were both, trace amounts of organic solvents and free un-cross linked plastics trapped within the film during fabrication, that were leaching out into the culture media and interfering with our cell culture viability. At any rate, introducing a "waiting" period between fabrication and using films as well as "soaking" them in aqueous solutions allowed us to substantially increase cell viability when cultured within the BCTB.

B) Adapt BCTB to include control of Acidic (pH) conditions within the same BCTB cartridge. (M 2-12)

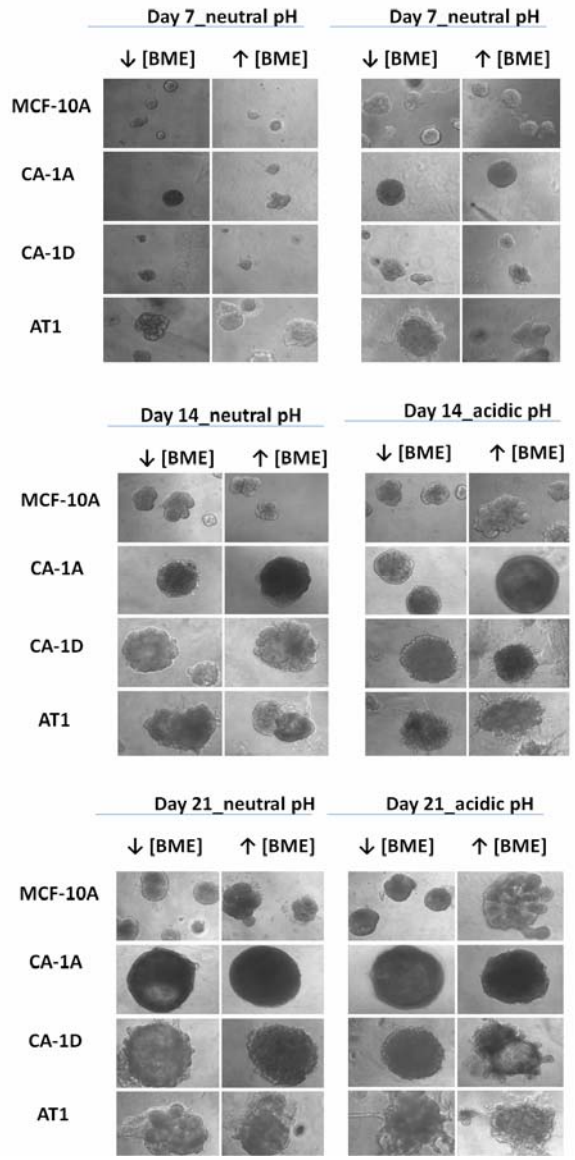

Figure 4. MCF-10A, -AT1, -CA1a and -10 CA1d cell line variants were cultured in the presence of standard (~3 mg/ml Matrigel) or High Concentration Basement Membrane (20 mg/ml). Cells were cultured in standard media for 7 days. At day 7, cells were transferred into either standard pH (7.4) media, or switched to low pH media (DMEM/F12 standard media + 10mM MES pH 6.6). Shown are representative images of mammosphere formation at 7, 14 and 21 days of culture.

i) Utilize microfluidic perfusion system to maintain pH within each biopsy/cell chamber.

Also, from Aim 1:Varying concentration of Matrigel to achieve differences in matrix stiffness.

As a test case for suitability of this system to maintain tissue viability, we previously compared mammosphere formation of MCF-10A cell lines and their variants in a chamber slide culture system (Nunc) that utilizes a thin slide compatible with confocal microscopy in parallel with cells cultured within our BCTB. In both cases cell chambers were coated with thin layer of Matrigel. Cells are resuspended in Matrigel ($3x10^5$ cells/ml) and plated into 8-well cell chamber (~70 µl/well) or bioreactor cell chamber (~7 µl/well) and allowed to gel for 1 hr at 37°C. Note that for the same resulting thickness of 3D gelled Matrigel in both systems, we are able to reduce our reagents consumption by a factor of 10 in the bioreactor as compared to the chamber slide. Cells are maintained in Growth Media consisting of DMEM/F12, 5% Horse Serum, 0.1 µg/ml insulin, 0.5 µg/ml hydrocortisone , 0.1 µg/ml cholera toxin, and 20 ng/ml EGF DMEM/F12, 5% Horse Serum, 0.1 µg/ml insulin, 0.5 µg/ml hydrocortisone , 0.1 µg/ml cholera toxin, and 20 ng/ml EGF. Cell cultures are maintained by either media changes every 3 days (8-well slide chamber) or with continuous perfusion in bioreactor.

We used this same system to begin applying variations in extracellular matrix composition within the BCTB. We are targeting traditional and "high" density specialized basement membrane ECM. We used our MCF10A and variant lines grown under organotypic conditions and compared mammosphere formation at 2 defined Matrigel/Basement

membrane extracellular matrix densities. Cells were seeded within 3D matrigel at low (3 mg/ml) or high (20 mg/ml) BME concentrations. Additionally, we are combining this with targeting "neutral" and "acidic/low" pH within our system. As we will begin to couple 3 different defined conditions within our BCTB (ECM densities, oxygen concentrations and pH levels), we compared neutral and acidic pH conditions on 2 distinct ECM densities grown under uniform, normoxic oxygen conditions.

Cells were seeded within 3D matrigel at low (3 mg/ml) or high (20 mg/ml) BME concentrations and mammospheres were allowed to form for 7 days using neutral pH buffered media (7.4 pH, standard media formulation). We tried 2 different types of assays. For one experimental assay set, shown in Figure 4, we established mammospheres under neutral media conditions and then either mainted this condition or switched a portion of mammospheres to low pH/acidic conditions. After 7 days of growth, half of the mammospheres cultures that were maintained in neutral pH buffered media (7.4 pH, standard media formulation)were transferred into DMEM/F12 standard media including 10mM MES that was 6.6 pH. In our preliminary findings we could visually see more "invasive" structures form in the low pH, high ECM growth conditions at day 14, but by 21 day of culture; however, we did not detect a change of growth characteristics.

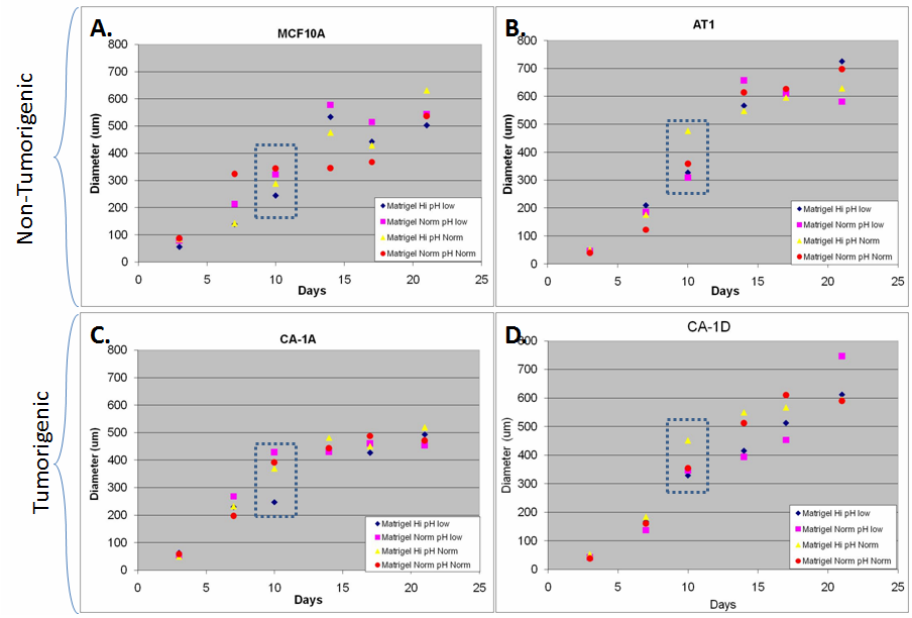

Figure 5. MCF-10A, -AT1, -CA1a and -10 CA1d cell line variants were cultured in the presence of standard (~3 mg/ml Matrigel) or High Concentration Basement Membrane (20 mg/ml) under either neutral or low pH media conditions. Cells were maintained in either standard pH (7.4) media, or low pH media (DMEM/F12 standard media + 10mM MES pH 6.6) throughout the 21 day culture period. Shown are average diameter of mammospheres at 3, 7, 10, 14, 17 and 21 days of culture. Blue: High Matrigel/Low pH; Pink: standard Matrigel/Low pH; Yellow: High Matrigel/Neutral pH; Red: Standard Matrigel/Neutral pH.

For a second experimental assay set, we seeded cells within 3D matrigel at low (3 mg/ml) or high (20 mg/ml) BME concentrations and mammospheres and immediately began growing cells in either neutral pH buffered media (7.4 pH, standard media formulation) or acidic pH buffered media (6.6 pH, DMEM/F12 standard media including 10mM MES). Interestingly, when mammospheres were cultured throughout under acidic conditions, there was an effect on mammosphere growth between 7 and 10 days of culture that was cell line dependent. For AT1 and CA-1D cell lines, the cells that

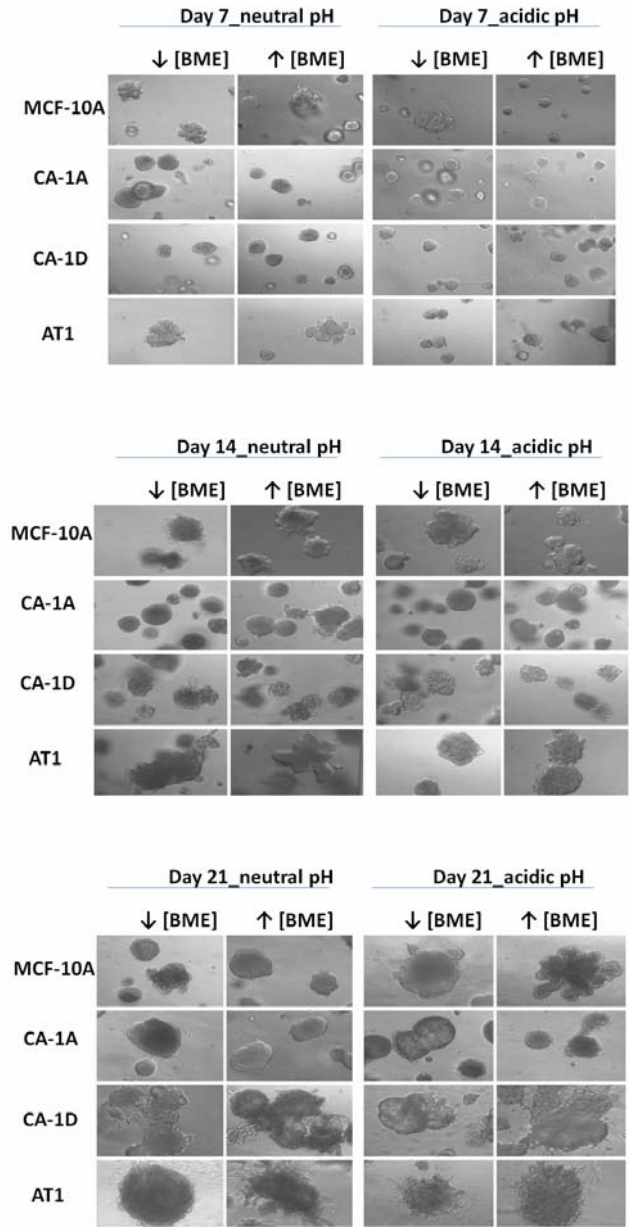

Figure 6. MCF-10A, -AT1, -CA1a and -10 CA1d cell line variants were cultured in the presence of standard (~3 mg/ml Matrigel) or High Concentration Basement Membrane (20 mg/ml) under either neutral or low pH media conditions. Cells were maintained in either standard pH (7.4) media, or low pH media (DMEM/F12 standard media + 10mM MES pH 6.6) throughout the 21 day culture period. Shown are representative images of mammosphere formation at 7, 14 and 21 days of culture.

were cultured under higher matrigel densities with neutral pH media, mammospheres formed larger mammospheres earlier than other grown conditions. Interestingly, MCF-10A and CA-1a cell lines differed, and indeed, the harsher high density BME with low pH was more restrictive of growth at that similar time point. This data is being used to standardize conditions within our BCTB culture system and in particular focusing our drug delivery investigations.

ii) Develop pH sensitive thin film which is chemically and optically compatible with previously developed (part A) oxygen sensitive film

Relying on our knowledge and experience gained during development of the oxygen sensitive film for 2D visualization of O_2 distribution within the BCTB, we have utilized a similar methodology to develop a pH sensitive thin film. Last year we reported on using a modified version of SNARF 5, SNARF®-5F 5-(and-6)-carboxylic acid, acetoxymethyl ester from Invitrogen, as a pH sensitive dye that was imbedded in Nafion film, which was spin - deposited on top of microscope slides. Initially, 50 μg of the dye were dissolved in 200 μL of a 50:50 mixture of acetone and methanol. Once the dye was dissolved, 2 mL of the 5% solution of Nafion were added to the mixture and allowed to sit for 1 h. Then, KW – 4A spinner (Chemat Technologies) was used to spin-coat 1"×2" microscope slides with 500 nm thick Nafion film containing pH dye. It was found that overnight stabilization of the film significantly improved its mechanical stability and adhesion to the glass substrate.

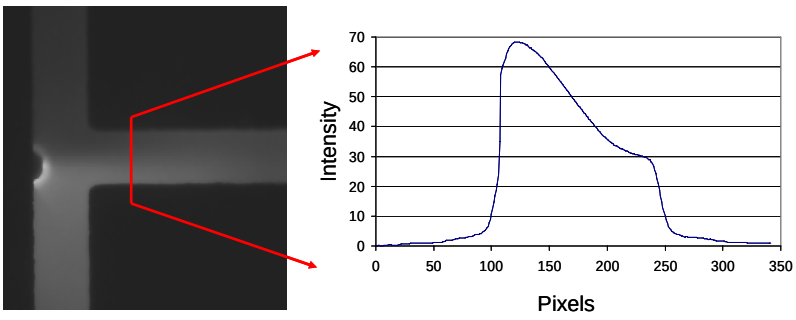

Figure 7. <u>Fluorescence and intensity line profile of the Nafion film containing SNARF-5F 5-(and-6)-carboxylic acid in the presence of buffers with pH 6 and pH 8</u>. Left) Observed changes in fluorescence of the pH film in response to pH 6 and pH 8 buffers flowing through the 100 mm wide microfruidic channel (Ex = 488 nm, Em = 575 / 40 nm). Right Panel) Line profile of the observed fluorescence signal across microfuidic channel as two buffers flow on top of pH sensitive film (40 pixel average along channel length).

While working on the development of the pH sensitive film, we have discovered that immobilization of the reporting molecules SNARF®-5F 5-(and-6)-carboxylic acid acetoxymethyl ester acetate (MW = 585.54 Da) from Invitrogen within the Nafion matrix slightly alters its optical properties. The pH dependent red shift in intensity (expected in free solution) was not observed as well as the pH-independent isosbestic point at 610 nm. The film showed excellent sensitivity to pH changes while illuminated with 488 nm and measuring fluorescence at 575 nm (without referencing to 610 nm isosbestic point). However, the prolonged exposure of the film to basic pH (8) buffer resulted in gradual deterioration of the fluorescence intensity. We attribute this to decomposition of the sensing molecule. Currently, we are testing a different, more stable reporter - SNARF®-5F 5-(and-6)-carboxylic acid (MW= 471.44 Da). Figure 7 shows the fluorescent image and a line profile across the microfluidic channel where pH6 and pH8 buffers merge into a single stream. The fluorescent properties of the new film are slightly different and characterized by reduced

auto-fluorescence outside the channel dimensions thus reducing the noise of present in the system. The long-term stability studies are underway.

Task 3. To determine whether drug response of a tumor biopsy sample evaluated within the BCTB predicts responsiveness in vivo using murine models of breast cancer.

Much of the work for this Task is published and presented in appendix A. Building off of our initial work using delivery of Matrix proteinase inhibitors to demonstrate long-term delivery of drug agents across long-term cell culture, we validated this through additional studies and also, we looked at delivery of docetaxel for 24 hrs and the effects on cell viability. Text that is Highlights of the work are taken from that work and appear below.

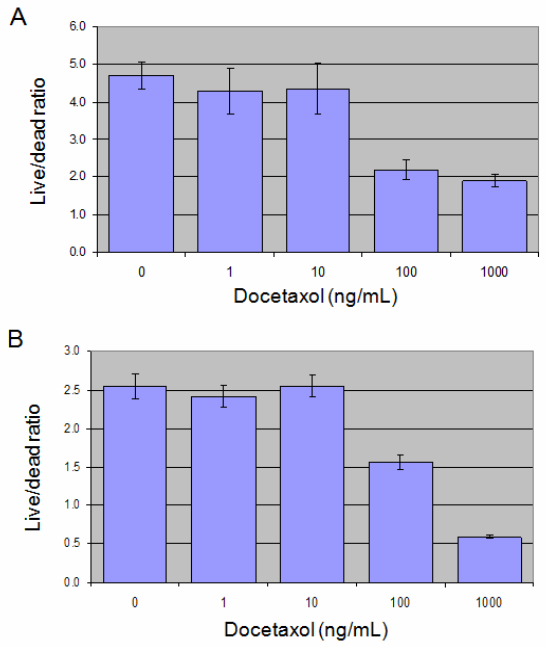

Figure 8. [also see appendix A, Supplemental Figure S6]. <u>Dose-dependent toxicity to increasing amounts of docetaxel affecting viability as evaluated by Live-Dead Viability Assay</u>.MCF-10 CA1d cells were cultured in (A) a cell culture chamber or (B) the TTB in the absence (0) or in the presence of docetaxel (10, 100, 1000 ng/ml). Following 24-hour incubation with docetaxel, the dose-dependent effect of docetaxel on cellular viability was evaluated by Live-Dead Viability Assay. Data are expressed as the ratio of Live (Calcein AM accumulation) to Dead (Ethidium) fluorescence staining. Data are expressed as Average Ratio ±SE (n=4).

Drug delivery within the TTB system. As a first step towards validation of drug delivery in our TTB, we applied increasing concentrations of a commonly used chemotherapeutic, docetaxel, for 24 hours to MCF CA1d cells within the TTB and a traditional 8-well culture chamber(14;15). Docetaxel treatment resulted in a dose-dependent increase in cell death of MCF-10 CA1d cells in both systems at concentrations that are commonly toxic to a wide range of cells (16;17).

As we were interested in monitoring cellular changes within a 3D organotypic microenvironment of a long-term cell culture system, we evaluated the ability of a known inhibitor to blunt cellular growth in our reactor system and compared results with our side-by-side tests using traditional cell culture techniques. Mammosphere formation is dependent upon a number of cellular processes and is regulated by extracellular proteinase activity. A matrix proteinase inhibitor cocktail known to target a broad spectrum of extracellular matrix proteinase activity was used (Aprotinin, for serine; GM6001, for metallo-; E-64, for cysteine; and Pepstain A, for aspartic; Calbiochem)(18). As we wanted to demonstrate long-term delivery of drug into our system, we first determined the amount of drug that could be continuously added to traditional cell culture without affecting long-term cell viability. For these experiments, we applied the matrix proteinase inhibitor cocktail to monolayer cell

cultures in incrementally higher concentrations and evaluated cell viability using the Live/Dead Assay (Molecular Probes). High concentration ranges of the proteinase inhibitor cocktail that have proven effective to inhibit cellular processes such as cellular migration are toxic to cells with 48 hours of continuous application (18); however, the concentration we chose for long-term drug delivery evaluation within the TTB system did not have an impact on cell viability (see Figure 8 or Appendix Supplemental Figure S7) yet retained its inhibitory properties.

Next, we assessed whether this non-toxic concentration of proteinase inhibitor cocktail was still effective as an extracellular matrix inhibitor within organotypic cell cultures. First, mammosphere formation of MCF-10A cells achieved with the traditional cell culture methods was blunted with addition of this non-toxic proteinase inhibitor cocktail (See Appendix Figure 4A). Second, we measured proteinase inhibition of proteinase activity in developing organotypic cultures within the TTB. For these experiments, we used the overlay method for establishing 6-day-old mammospheres. Additionally, because it is known that reduced growth factor Matrigel contains trace matrix proteinase content, and because we wanted to improve the baseline sensitivity of the proteinase activity assay, we cultured the MCF-10A cells and variants in a Matrigel:hydrogel mixture. The defined artificial matrix (*i.e.,* hydrogel) contains low endogenous proteolytic activity that allowed for visualization of cell-associated proteolytic activity. The 1:1 mixture did not affect long-term mammosphere formation within the time frame evaluated. Following 6 days of culture, mammospheres were overlaid with hydrogel containing fluorogenic probe (DQ-gelatin). The mammospheres were cultured in the presence and absence of matrix proteinase inhibitor cocktail for 48 hours. As shown in Appendix Figure 4B, MCF-10AT1 organotypic cultures demonstrated robust proteinase activity, as indicated by the increase of fluorescein fluorescence of the matrix-embedded DQ-gelatin. However, there was a notable reduction in proteinase activity surrounding mammospheres cultured in the presence of proteinase inhibitors. Our results demonstrate effective protease inhibition using these concentrations of the proteinase inhibitor cocktail.

We next evaluated long-term drug delivery within the TTB. Using organotypic cultures of the MCF-10A human mammary epithelial cell line and their invasive counterparts grown within the TTB, we assessed mammosphere formation in the absence and presence of continuous application of the protease inhibitor cocktail that targets a broad spectrum of extracellular matrix proteinase activity into the system. As shown in Appendix Figure 5, this protease inhibitor cocktail down-regulated morphogenesis of the MCF-10A variants within the TTB. MCF-10A cell lines showed on average a ~32% reduction in mammosphere diameter, whereas the MCF-10 -AT, -CA1a, and -CA1d demonstrated a more robust average reduction in mammosphere diameter of ~ 73%, 61%, and 67%, respectively.

Interestingly, the sensitivity of the proteinase inhibitory effects correlates well with endogenous matrix proteinase activity of these cell lines. Conditioned media collected from MCF-10A and MCF-10 -AT, -CA1a, and -CA1d grown under 2D monolayer culture conditions was compared for its ability to cleave denatured collagen (*i.e.,* DQ-gelatin). MCF-10A had the lowest measureable endogenous matrix proteinase degrading ability at a rate of 112.2 ± 22.4 (AU/min± SE). MCF-10 -AT, -CA1a, and -CA1d cell line variants had higher rates of measured degradation ability at 168.2±18.8, 123.2±27.8, and 169.7±31.3 (AU/min± SE). Since the endogenous proteinase activity for MCF-10A is less when compared to its tumorigenic variants, it would be logical to expect that the decrease in mammosphere size would also be the least out

of the whole cell panel. Overall, these results suggest that *in vitro* acinar development and the subsequent down-regulation of mammosphere formation were correlated with pharmacological down-regulation of matrix proteinase activity in these cell systems. Additionally, our results are supported by a short, 5-day 3D static culture of T47D breast carcinoma cells in collagen inside a microfluidic channel (19), where a 45% decrease in the size of cell clusters formed was observed after the incubation with a single MMP inhibitor GM6001. In general, our studies demonstrate the utility of the TTB for long-term organotypic culture and continuous drug delivery within a closed system with capabilities for optical analysis of cellular functions.

KEY RESEARCH ACCOMPLISHMENTS: Bulleted list of key research accomplishments emanating from this research.

- BCTB Modular design: each reactor can be maintained under different flow (nutrient exchange) profile or connected to a single supply source via manifolds
- Manifolds in combination with gravity induced flow are effective low cost approach to passively regulate the perfusion rates through BCTB
- System is capable to maintain long-tern (>20 days) cellular viability and allows for proper formation of mammospheres
- System allows for efficient delivery of a treatment as was confirmed by short term dose dependent toxicity with increasing docetaxel concentration and also by inhibition of mammosphere formation and proteinase activity (long-term dose).
- There is a significant difference in oxygen delivery into BCTB between plasma treated and native PDMS
- After 3 day aging, the diffusion coefficient of O_2 in PDMS is restored close to the original, untreated value when maintained in air. If the surface remains in contact with aqueous solutions (culture media) the recovery rate is significantly reduced (3 weeks). Even though highly cross-linked PDMS has the same permeability in the untreated state, it remains significantly less permeable to O_2 even 3 weeks after the plasma treatments
- New, more stable version of pH sensitive dye has been adopted.
- Oxygen and pH sensitive film for 2D mapping of O_2 and pH distribution, respectively, within the BCTB have been developed. With proper preparation, Oxygen Sensitive film is compatible with standard cell culture and gamma ray sterilization methods.
- Mammosphere formation under varying pH and BME density has been accomplished with cell line specific distinct growth characteristics noted.

REPORTABLE OUTCOMES:

Meeting Report

1. LJ McCawley, JQ. Lu, E.M. Lillie, and D.A. Markov Breast Cancer Tissue Bioreactor For Direct Interrogation And Observation Of Response To Antitumor Therapies, Era of Hope Meeting, DOD/BCRP, Orlando Fl, 2011

2. D.A. Markov, E. Lillie, J.Q. Lu, P. Samson, J.P. Wikswo, and L.J. McCawley, "Development of the Bioreactor system for maintaining native tumor tissue microenvironment", *Vanderbilt Postdoctoral Research and Shared Resources Symposium*, Nashville, TN 2011 (1st place Prize)
3. D.A. Markov, E. Lillie, J.Q. Lu, P. Samson, J.P. Wikswo, and L.J. McCawley, "*Ex vivo* bioreactor system to mimic native tumor tissue microenvironment" *VICC Symposium*, Nashville, TN 2011

Manuscript

1. Markov DA, Lu JQ, Samson P, Wikswo JP, and McCawley LJ. Thick-tissue bioreactor as a platform for long term organotypic culture and drug delivery. Lab Chip, 21(12):4560-8, 2012. PMID: 22964798

CONCLUSION:

As a major investment towards our overall goal, we focused on a manuscript this year discussing our development of a breast cancer tissue bioreactor (BCTB) capable of sufficient nutrient supply and metabolite exchange for thick tissue culture in microfluidic environment and that could deliver an inhibitor of a cellular process that would impact cellular growth. Last year, we described our development of a drug delivery regimen and applied this within our portable BCTB that is capable of maintaining sterile microenvironment and sustaining cell growth, maturation, and organ formation during three week long cell culture. The performance of drug delivery within the BCTB was validated with MCF10A cell line and its tumorigenic variants that have developed into hollow lumen spheroids in 21 days. Real-time staining and visualization of fully developed mammospheres was possible within the closed bioreactor system. Fully assembled TTB was compatible with regular and fluorescent microscopy and allowed for optical assessment of the mammospheres development and proteinase activity using conflocal microscopy. We applied a proteinase inhibitor regimen and could monitor the concomitant inhibition of mammosphere morphogenesis. We focused this past year on performing enough replicates to validate drug delivering and growth performance; and additionally measured diameter of mammospheres formed to assess the effects of drug agents on growth inhibition of mammosphere formation. Additionally, we contrasted matrix proteinase activity in the cell lines, demonstrating that the cell lines with the highest matrix proteinase activity were more sensitive to growth inhibition as determined by changes in mammosphere size at the end of the study. Furthermore, we assessed delivery of docetaxel into the system and measured effects of docetaxel on viability of MCF-CA1d cells, demonstrating a dose dependent effect on cell viability using our BCTB that was comparable to use of standard tissue culture dishes but with reduced reagents

We have developed thin film sensors to monitor oxygen states within the fully developed BCTB. As we began to move forward to apply these oxygen thin films to monitor oxygen delivery to cells in culture, we noted effects on cell viability with prolonged (over 24 hours). Through various testing, we speculate that there were both, trace amounts of organic solvents and free un-cross linked plastics trapped within the film during fabrication, that were leaching out into the culture media and interfering with our cell culture viability. We have a new protocol of thin film handling that led to substantially improved cell viability when used with cultures within the BCTB. Furthermore, we are working towards improving stability of our thin film sensors to monitor pH states within the fully developed BCTB.

We have have started a thorough assessment of mammosphere formation under different environmental conditions, focusing on distinct matrix densities and pH conditions. We have noted a distinct difference in growth rates between the panel of cell lines as well as the microenvironmental conditions. Importantly, these conditions will be exploited as we test drug inhibition in our BCTB chamber and assess both mammosphere formation, as well as determining sensitivity of biopsy material to drug treatment ex vivo as compared to in vivo treatment of these same tumor types to therapy.

Our goal is to engineer a Breast Cancer Tissue Bioreactor will maintain the in vivo functionality a patient's tumor biopsy sample ex vivo and be used to screen response to anti-tumor agents, such that the patient's own tumor tissue can be used to predict that best therapeutic treatment option for that individual patient. The conditions in the tumor microenvironment affect cellular functionality of the cell types within, including the effectiveness and response to anti-cancer therapeutics. Thus, we believe that the predictability of the patient's response to chemo- or molecular therapeutics will require an exact mimicry of the in vivo tumor microenvironmental conditions. The purpose of the devices and technologies described herein is to perfect a novel small scale bioreactor that allows unprecedented control over specifying the exact environmental conditions to maintain a breast tumor biopsy sample, thus allowing recapitulation ex vivo of the typical tumor microenvironment. We have laid down a foundation and design rules for future reactor developments as we implement the BCTB with controlled oxygenation and pH states for maintenance of tumor biopsy samples. It would be beneficial to develop a microfluidic device that would be compatible with 3D organotypic cell culture and capable of maintaining tumor biopsy specimen for extended periods of time in its natural 3D microenvironment allowing for testing of various treatment options in order to select the most optimum for the patient.

REFERENCES:

Reference List

1. Gatenby RA, Gillies RJ. A microenvironmental model of carcinogenesis. Nat.Rev.Cancer 2008 Jan;8(1):56-61

2. Gatenby RA, Smallbone K, Maini PK, Rose F, Averill J, Nagle RB, Worrall L, Gillies RJ. Cellular adaptations to hypoxia and acidosis during somatic evolution of breast cancer. Br.J.Cancer 2007 Sep 3;97(5):646-53

3. Smallbone K, Gavaghan DJ, Gatenby RA, Maini PK. The role of acidity in solid tumour growth and invasion. J.Theor.Biol. 2005 Aug 21;235(4):476-84

4. Lundgren K, Holm C, Landberg G. Hypoxia and breast cancer: prognostic and therapeutic implications. Cell Mol.Life Sci. 2007 Dec;64(24):3233-47

5. Tredan O, Galmarini CM, Patel K, Tannock IF. Drug resistance and the solid tumor microenvironment. J.Natl.Cancer Inst. 2007 Oct 3;99(19):1441-54

6. Chan N, Koritzinsky M, Zhao H, Bindra R, Glazer PM, Powell S, Belmaaza A, Wouters B, Bristow RG. Chronic hypoxia decreases synthesis of homologous recombination proteins to offset chemoresistance and radioresistance. Cancer Res. 2008 Jan 15;68(2):605-14

7. Zhang Y, Li M, Yao Q, Chen C. Recent advances in tumor hypoxia: tumor progression, molecular mechanisms, and therapeutic implications. Med.Sci.Monit. 2007 Oct;13(10):RA175-RA180

8. Sarkaria JN, Bristow RG. Overview of cancer molecular radiobiology. Cancer Treat.Res. 2008;139:117-33

9. Heldin CH, Rubin K, Pietras K, Ostman A. High interstitial fluid pressure - an obstacle in cancer therapy. Nat.Rev.Cancer 2004 Oct;4(10):806-13

10. Cairns R, Papandreou I, Denko N. Overcoming physiologic barriers to cancer treatment by molecularly targeting the tumor microenvironment. Mol.Cancer Res. 2006 Feb;4(2):61-70

11. Markov DA, Lu JQ, Samson PC, Wikswo JP, McCawley LJ. Thick-tissue bioreactor as a platform for long-term organotypic culture and drug delivery. Lab Chip 2012 Nov 7;12(21):4560-8

12. Amao Y, Miyashita T, Okura I. Platinum tetrakis(pentafluorophenyl)porphyrin immobilized in polytrifluoroethylmethacrylate film as a photostable optical oxygen detection material. Journal of Fluorine Chemistry 2001 Jan;107(1):101-6

13. Borisov SM, Wolfbeis OS. Optical biosensors. Chem.Rev. 2008 Feb;108(2):423-61

14. Crown J, O'Leary M, Ooi WS. Docetaxel and paclitaxel in the treatment of breast cancer: a review of clinical experience. Oncologist. 2004;9 Suppl 2:24-32

15. Ward S, Simpson E, Davis S, Hind D, Rees A, Wilkinson A. Taxanes for the adjuvant treatment of early breast cancer: systematic review and economic evaluation. Health Technol.Assess. 2007 Oct;11(40):1-144

16. Hernandez-Vargas H, Palacios J, Moreno-Bueno G. Telling cells how to die: docetaxel therapy in cancer cell lines. Cell Cycle 2007 Apr 1;6(7):780-3

17. Morse DL, Gray H, Payne CM, Gillies RJ. Docetaxel induces cell death through mitotic catastrophe in human breast cancer cells. Mol.Cancer Ther. 2005 Oct;4(10):1495-504

18. Wolf K, Mazo I, Leung H, Engelke K, Von Andrian UH, Deryugina EI, Strongin AY, Brocker EB, Friedl P. Compensation mechanism in tumor cell migration: mesenchymal-amoeboid transition after blocking of pericellular proteolysis. J Cell Biol. 2003 Jan 21;160(2):267-77

19. Bauer M, Su G, Beebe DJ, Friedl A. 3D microchannel co-culture: method and biological validation. Integr.Biol. 2010;2(7-8):371-8

Appendix

1. Markov DA, Lu JQ, Samson PC, Wikswo JP, McCawley LJ. Thick-tissue bioreactor as a platform for long-term organotypic culture and drug delivery. Lab Chip 2012 Nov 7;12(21):4560-8

See Attached.

Lab on a Chip

Accepted Manuscript

This is an *Accepted Manuscript*, which has been through the RSC Publishing peer review process and has been accepted for publication.

Accepted Manuscripts are published online shortly after acceptance, which is prior to technical editing, formatting and proof reading. This free service from RSC Publishing allows authors to make their results available to the community, in citable form, before publication of the edited article. This *Accepted Manuscript* will be replaced by the edited and formatted *Advance Article* as soon as this is available.

To cite this manuscript please use its permanent Digital Object Identifier (DOI®), which is identical for all formats of publication.

More information about *Accepted Manuscripts* can be found in the **Information for Authors**.

Please note that technical editing may introduce minor changes to the text and/or graphics contained in the manuscript submitted by the author(s) which may alter content, and that the standard **Terms & Conditions** and the **ethical guidelines** that apply to the journal are still applicable. In no event shall the RSC be held responsible for any errors or omissions in these *Accepted Manuscript* manuscripts or any consequences arising from the use of any information contained in them.

RSC Publishing

www.rsc.org/loc
Registered Charity Number 207890

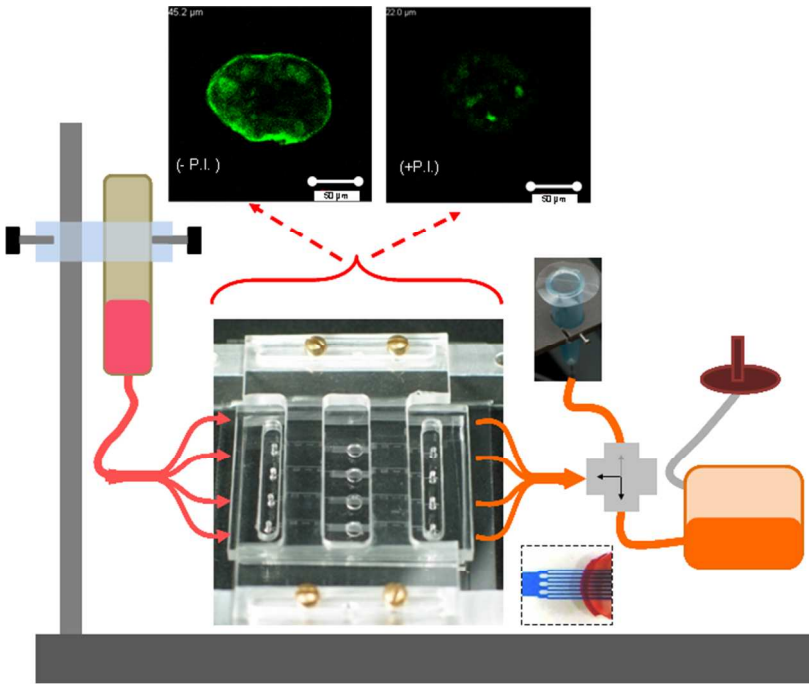

Thick Tissue Bioreactor system for long-term organotypic on-chip cultures and reagent delivery to tissue-like cell densities within low-volume microenvironment

Thick-tissue bioreactor as a platform for long-term organotypic culture and drug delivery

Dmitry A. Markov [a,b], Jenny Q. Lu [a,b], Philip C. Samson[b,d], John P. Wikswo[b,c,d,e], and Lisa J. McCawley [a,b]

[a] *Department of Cancer Biology, Vanderbilt University Medical Center, Nashville, TN 37232, USA*
[b] *Vanderbilt Institute for Integrative Biosystems Research and Education, Vanderbilt University, Nashville, TN 37235, USA*
[c] *Department of Molecular Physiology and Biophysics, Vanderbilt University Medical Center, Nashville, TN 37232, USA*
[d] *Department of Physics and Astronomy, Vanderbilt University, Nashville, TN 37235, USA*
[e] *Department of Biomedical Engineering, Vanderbilt University, Nashville, TN 37235, USA*

Abstract

We have developed a novel, portable, gravity-fed, microfluidics-based platform suitable for optical interrogation of long-term organotypic cell culture. This system is designed to provide convenient control of cell maintenance, nutrients, and experimental reagent delivery to tissue-like cell densities housed in a transparent, low-volume microenvironment. To demonstrate the ability of our Thick-Tissue Bioreactor (TTB) to provide stable, long-term maintenance of high-density cellular arrays, we observed the morphogenic growth of human mammary epithelial cell lines, MCF-10A and their invasive variants, cultured under three-dimensional (3D) conditions inside our system. Over the course of 21 days, these cells typically develop into hollow "mammospheres" if cultured in standard 3D Matrigel. This complex morphogenic process requires alterations in a variety of cellular functions, including degradation of extracellular matrix that is regulated by cell-produced matrix proteinases. For our "drug" delivery testing and validation experiments we have introduced proteinase inhibitors into the fluid supply system, and we observed both reduced proteinase activity and inhibited cellular morphogenesis. The size inhibition results correlated well with the overall proteinase activities of the tested cells.

Key words:

microfluidic, bioreactor, bioMEMS, organotypic cell culture, long-term cell culture, breast cancer, proteinase activity, mammosphere, MCF-10A, organ-on-chip

Abbreviations:

3D: three-dimensional

PDMS: polydimethylsiloxane

TTB: Thick-Tissue Bioreactor

TURN: Tape Underlayment Rotary Node

ECM: extracellular matrix

MSC: mesenchymal stem cell

MMP: matrix metallo-proteinase

PI: proteinase inhibitor

RF: radio frequency

Introduction

Traditional cell culture approaches that use monolayer culture within tissue culture dishes or well plates cannot recreate the complex chemical and physical microenvironment that exists in tissue. In addition, cells themselves are in constant communication with each other and the surrounding matrix, modifying it or modifying their own behavior based on the changes in their adjacent microenvironment(1). Realistic assessment of cellular processes regulating tumorigenesis and particularly of *in vitro* anti-cancer treatments must take both cell-cell and cell-matrix components into account. Furthermore, culturing cells within three-dimensional (3D) systems facilitates cellular growth that better recapitulates *in vivo* cellular behavior, molecular functions, and gross morphological features(2;3). Moreover, cellular response to perturbations in the system, such as application of anti-tumor therapeutics, can differ depending upon the culture system used. For instance, in MCF-7 cancer cell lines it has been shown that the effectiveness of anti-tumor treatments on cells that were cultured in 3D matrix was reduced by orders of magnitude compared to the treatments on the same cells cultured in a monolayer(4;5). There is an obvious need to develop cell culture techniques incorporating three-dimensional matrix, where both chemical and physical microenvironments more closely approximate physiological conditions. It is also important for these 3D culturing systems to competently provide cell maintenance conditions over time spans of several weeks in order to allow completion of cellular morphogenic programs(2;3;6).

In recent years multiple approaches have been developed that employ microfluidic devices to recreate the 3D microenvironment *in vitro* and to grow large populations of cells at tissue-like densities(7). Microfluidic technology and devices applied to cell culture offer important advantages over standard culture techniques. There is significant reduction in size and

in reagent use; cells can potentially be cultured at higher densities with more realistic cell-to-fluid volume ratios that do not dilute paracrine and autocrine factors; media flows are laminar and the flow rates can be easily adjusted in real-time for proper delivery of media, proteins, or assay reagents; and various spatial and temporal chemical gradients can be established within the microfluidic cell culture devices(8;9). Our group is focused on developing a microfluidics-based bioreactor for three-dimensional long-term culture of large populations of cells or small portions of excised tissue in a controlled microenvironment.

There have been several approaches used in the development of microfluidics-based cell culture bioreactors that address issues of long-term culture, the majority of which concentrate on interrogation of cells growing in a monolayer for up to 12 days. However, as *in vitro* monolayer cultures do not always faithfully mimic cellular *in vivo* behavior, the current trend is to grow cells in a more "natural," tissue-like, 3D microenvironment, while still utilizing the advantages afforded by microfluidics. Even though this new technology is still under development, it has been successfully applied to maintaining viability of tumor spheroids for several hours for cancer treatment screening(10), monitoring the weeks-long process of differentiation from myoblasts to myotubes(11), and observing adipogenic and osteogenic differentiation of mesenchymal stem cells (MSCs)(12). Some groups have attempted to construct microfluidic bioreactors suitable for maintaining proper functionality of small tissue samples for periods of time ranging from a couple of hours to 3 days(13). Dhurjati *et al.*(14) introduced a large-format microfluidic bioreactor (25 cm^2 culture area) within which fetal osteoblasts were cultured uninterrupted for four months (120 days). Bauer *et al.*(15) used collagen-filled PDMS microchannel plates(16) and similarly filled commercial polystyrene microchannel plates to grow 3D co-cultures of human mammary fibroblasts and T47D breast carcinoma cells for 5 days, and demonstrated the effects

of inhibition of paracrine signaling on fibroblast-induced carcinoma cell mitogenesis. All of these systems performed well for the intended purpose; however, many needed expensive external active fluid-pumping sources, and some required complex multilayer assembly, *e.g.,* 10 layers(17), or additional mechanisms to provide shear stresses.

Our Thick-Tissue Bioreactor (TTB) is a compact, stand-alone, gravity-fed microfluidic system that 1) can be easily sterilized, assembled under sterile conditions, and transported between culture incubator and the imaging station; 2) maintains cell viability for long-term cell culture, with the future goal of long-term maintenance of tissue (*i.e.*, tumor) biopsy samples; and 3) allows convenient visualization of the response of cells and tissues to drug agent challenges. To validate the suitability of our custom-built TTB to maintain long-term organotypic culture and regulate drug delivery, we utilized the long-term culture and morphogenic program of breast epithelial cell lines, MCF-10A and their invasive and tumorigenic variants (MCF-AT1 and MCF-CA1d), grown in 3D gelled tissue matrix (*i.e.*, Matrigel)(6;18). The MCF-10A human mammary epithelial cell lines undergo a distinct morphogenesis pattern that results in the formation of hollow "mammospheres" in standard 3D Matrigel culture systems over the course of 21 days(6). This complex process requires alterations in a variety of cellular functions, including proliferation, migration, matrix degradation, and cell survival, making this a useful system for testing a long-term cell culture bioreactor and the long-term effects of inhibitory agents, such as matrix proteinase inhibitors, targeted towards regulating these cellular processes. Validation of drug delivery into the system was accomplished by applying matrix proteinase inhibition to the system to impair the morphogenic process and compare it against mammosphere formation in the absence of proteinase inhibition.

Materials and Methods

Design and fabrication of Thick-Tissue Bioreactor (TTB). The Thick-Tissue Bioreactors (TTB) were fabricated in polydimethylsiloxane (PDMS) using standard soft lithography and replica molding techniques. The device consists of two parts: 1) a 1 mm thick PDMS membrane that contains four Cell/Biopsy growth chambers that are 3 mm in diameter and separated by 5.85 mm, and 2) a 4 mm thick PDMS top piece that contains four microfluidic supply networks, one for each chamber (Figure 1A and B). The cell culture membrane is bonded to a 2" x 3", 1 mm thick glass slide to provide structural support and to allow cell imaging through an inverted microscope. Growth chambers are in direct contact with supply networks or, alternatively, are separated from microfluidic supply channels by a polycarbonate filter (Osmonics, Inc.) with 0.4 μm pores, which maintains diffusional exchange of nutrients and waste products and prevents leakage of extracellular matrix (ECM) into the microfluidic channels. These pores are too small to allow cell migration. The supply network for each of the cell growth chambers consists of eight parallel microfluidic channels 100 μm wide × 100 μm tall, separated by 100 μm walls. These are connected together to larger 800 μm wide input / output regions of the network (shown in blue in Figure 1A and B). Splitting a larger supply channel for each of the cell culture chambers into several parallel paths allows maintenance of structural integrity of the supply network, prevents possible channel collapse during the reactor assembly and clamping, and provides alternative pathways for the perifusing media in case some of the Matrigel escapes and blocks one of the smaller channels. The entire reactor is clamped together under sterile conditions in a custom-built polycarbonate and stainless steel clamp that allows for easy alignment of the reactor components, provides structural stability to the assembly, and evenly distributes holding pressure across the PDMS surfaces (Figure 1C and D).

All four individual reactors in a single TTB cartridge are gravity-fed from a modified 14 mL tube with a loose-fitting cap (*i.e.*, a "snap cap tube") mounted in a custom-built holder. We described previously our modifications to the tube (19). The output of the feeding tube is directly connected to a manifold assembly containing 100 μm wide and 50 μm tall microfluidic channels that split the input flow into four even streams for each of the reactors within the cartridge. A second output manifold (on the waste side of the reactor) is used as in-series fluid flow resistance to passively regulate the flow rate, to recombine the outflow from four reactors, and to direct effluent into a waste collector (Labtainer™ from HyClone) or, alternatively, to sample extraction systems (Figure 1D and E) that collect fluid while preventing retrograde contamination of the reactor(19). The fluid level in the feeding tube was typically checked daily and replenished every other day to be maintained at 15 cm above the bioreactor surface. All tubing was 0.020" ID, 0.060" OD Saint-Gobain Tygon microbore tubing (Part # AAQ04103) from Fisher Scientific.

Bioreactor assembly and clamping. The PDMS membrane with cell chambers resting on a glass slide were sterilized by autoclaving, and the remaining partially assembled bioreactor components (clamps, lids, supply networks, tubing, etc.) were sterilized using gamma irradiation. Other sterilization methods were tested and abandoned because ethanol and ethylene oxide readily partition into plastic components(20), and autoclaving is not suitable for the assemblies containing materials with drastically different coefficients of thermal expansion. The 2 partially assembled reactor portions (illustrated in Supplemental Figure S1) allowed for ease in loading the 3D matrix and cell components and the subsequent easy alignment and combination of the two portions into a complete system. The sterilized individual TTB components were fully assembled in a standard cell culture biosafety laminar flow hood using standard aseptic techniques with care to maintain the sterile conditions of the internal working components of the

TTB that are in contact with cells and media. After the cell chambers were loaded with Matrigel/cell mixture, they were initially sealed using the top PDMS piece, which contains the microfluidic supply network with dry channels, to avoid possible cross-contamination between the four adjacent cell growth chambers, and also to avoid the possibility of trapping air bubbles in the supply channels. Next, the glass slide containing the loosely sealed bioreactor components was clamped in position via a pressure plate and a lid, which was securely attached to the pair of stainless steel holders with 4-40 stainless steel screws. Both the lid and the pressure plate were machined from ¼" thick abrasion-resistant polycarbonate plate purchased from McMaster-Carr (Part # 8707K131).

Cell lines and culture. MCF-10A and MCF-10A pBabe (vector control) cell lines were obtained from Joan Brugge (Harvard Medical School, Boston, MA)(6). Ras-transformed MCF-10AT1 and the tumorigenic MCF-10CA1a and MCF-10CA1d variants were obtained from Dr. Fred Miller (Barbara Ann Karmanos Cancer Center, Wayne State University, Detroit, MI)(18). These MCF-10A and cell line variants form varying degrees of invasive structures in 3D Matrigel, depending upon the degree of transformation and tumorigenicity of the cell line. Cells were maintained in "Growth Media" (DMEM/F12, 5% horse serum, 0.1 µg/ml insulin, 0.5 µg/ml hydrocortisone, 0.1 µg/ml cholera toxin, and 20 ng/ml EGF) unless specified otherwise.

3D Matrigel culture/mammosphere formation. All cell culture experiments were done in parallel using both our TTB bioreactors and standard 8-well chamber slide cell culturing techniques. Cell chambers of both the TTB bioreactor systems and the 8-well chamber slide were coated with 2 µl and 30 µl of low growth factor Matrigel, respectively. Then the cells were re-suspended in Matrigel ($3x10^5$ cells/ml) and plated into bioreactor cell chambers (~5 µl/well) or 8-well cell chambers (~70 µl/well) and allowed to gel for 1 hour at 37°C. Based on chamber

dimensions, these volumes of Matrigel resulted in an equal thickness of 1 mm for both culture systems. Cells were maintained with Growth Media by either media changes every 3 days (8-well chamber) or continuous perifusion in the bioreactor. Mammospheres were cultured in the absence or presence (when indicated) of the following 1x proteinase inhibitor (PI) cocktail: 12.5 μM GM-6001 (metallo-); 125 μM E-64 (cysteine); 50 μM Pepstatin A (aspartate); 1 μM Leupeptin (cathepsin D); 1.1 μM Aprotinin (serine).

Drug toxicity measurements. For MCF-10 CA1d cell monolayer drug toxicity testing using docetaxel, 1.0 x 10^4 cells were plated into each TTB cell chamber and 3.0 x 10^4 cells/well into an 8-well chamber slide. Cells were cultured with increasing concentrations of docetaxel (0, 1, 10, 100 and 1000 ng/ml) as indicated for 24 hours. For establishing the threshold of non-toxicity of the proteinase inhibitor cocktail, we plated MCF-10A cells and cell line variants into 8-well chamber slides (5000 cells/chamber), and treated them in the absence or presence of increasing concentrations of the proteinase inhibitor cocktail (0.5 x, 1x and 2x) for 48 hours. We assessed cell viability using Live/Dead Assay (Molecular Probes) according to manufacturer's directions, using 1μM of Calcein AM (*i.e.,* live stain indicator) and 2 μM of Ethidium homodimer-1 (*i.e.,* dead stain indicator).

Protease activity measurements. Mammospheres were first established for 6 days using a modified overlay method(6). Briefly, after laying down a plug of 1:1 Matrigel/BD Puramatrix Peptide Hydrogel (BD Biosciences) mixture in both the bioreactor (2 μl) and 8-well (10 μl) cell chamber systems, cells (3x10^5 cells/ml) were plated into the bioreactor cell chamber (500 cells/5 μl Matrigel:hydrogel mixture/well) or the 8-well cell chamber (5000 cells/20 μl Matrigel:hydrogel mixture/well) and allowed to gel for 1 hour at 37°C. Cells were cultured for 6 days to form mammospheres in phenol red free Growth Media containing 2% of Matrigel. To

assess proteinase activity, on day 6 the media was aspirated and mammospheres were overlaid with 25 μg/mL of DQ gelatin (Ex/Em 495/515 nm; Molecular Probes) in peptide hydrogel. Following 48 hours of incubation, we assessed protease activity by the increase of fluorescence detected using a Zeiss LSM 510 scanning confocal microscope.

Phalloidin and real-time SYTO-63 staining. To visualize mammosphere formation of live cell cultures, *in situ*, cell nuclei were stained using 1:5000 dilution of Syto 63 (Molecular Probes). Alternatively, mammospheres were fixed at set time points with 10% buffered formalin and stained using 1:400 dilution of phalloidin in 0.5% Triton-X and 1:3500 of Hoescht to visualize nuclei. A 1 mL syringe of diluted fluorophore was pumped through the parallel channels and incubated for 1 hour, after which the reactor system was washed with 1 ml of 1X PBS. The PBS-filled tubing was closed with Luer-lock stoppers. Confocal images within bioreactors were taken with a Zeiss LSM 510 scanning confocal microscope.

Determination of extracellular matrix proteinase activity. Media from MCF-10A and cell line variants cultured to confluence in 100 mM plates was replaced with serum-free experimental buffer (DMEM/F12 containing 5 ng/ml EGF/ 10 μg/ml Insulin), and conditioned media was collected following 48 hours of incubation. 1/10 total volume was concentrated and analyzed for the ability to cleave 3 mMol dye-quenched (DQ)-gelatin (Molecular Probes) in Zn^{2+}/Ca^{2+} Tricine buffer (50 mM Tricine, pH 7.4, 0.2 M NaCl, 10 mM $CaCl_2$, 50 μM $ZnSO_4$ and 0.005% Brij 35) in the absence and presence of the protease inhibitor cocktail (2.2 μM Aprotinin, 25 μM GM-6001, 250 μM E-64, 100 μM Pepstatin A and 2 μM Leupeptin; Calbiochem)(21). Fluorescence (excitation: 485 nm; emission: 538 nm) was measured at 37°C, as a function of time using an MFX Microtiter Plate Fluorometer (Dynex Technologies, Inc., Chantilly, VA). Fluorometric measurements were used to calculate an initial rate of enzyme

activity (Δ fluorescence units/minute). As a positive control, DQ-Gelatin was cleaved to completion with 10 ng active-MMP-9.

Determination of microfluidic flow rates. Flow measurements through the TTB were made using the NanoFlow sensor from IDEX Health & Science (formerly, Upchurch Scientific) with a sampling rate of 2 Hz. The NanoFlow sensor was delivered pre-calibrated from the supplier, and the flow rate was confirmed using precision syringe pumps. Tests were performed on a fully assembled system (without cells) inside a custom-built chamber at a constant temperature of 37°C and 100% humidity, mimicking conditions inside the tissue culture incubator. The basic technology for regulating flow through the device involved 1) a fixed height of the gravity supply reservoir and 2) experimental determination of the required fluid resistance offered by the 4-way input splitter manifold in conjunction with the fluid resistance offered by the 4-way output combiner manifold. The 50 μm height of the input manifold microchannels was chosen to provide sufficient fluid resistance to ensure passive volume sharing between the four supply channels of the bioreactor array. To provide a reproducible method of varying bioreactor fluid flow between different experiments, we fabricated a number of different output manifolds, each with the same topology and the same 100 μm channel width as the input manifold but with different channel heights (range 5-60 μm). By selecting an appropriate output manifold we could provide calibrated fluid flow to the bioreactor. The head pressure was kept constant at 15 cm (see Figure 2).

Addressing possible partitioning of molecules into the PDMS bioreactor walls. We used Rhodamine B, a water soluble dye well known to partition into PDMS(22), to evaluate various methods of treating PDMS microfluidics surfaces in order to minimize the possible absorption of bioactive molecules. Microfluidic channels 50 μm tall and 50 μm wide were

fabricated using soft lithography and replica molding as described above. A set of 8 channels was molded in a circular Petri dish from the same wafer with the same batch of PDMS mixed at the same time. After curing in the oven at 65°C overnight, rectangular blocks of PDMS containing 2 channels each were cut out, access holes were punched, and the devices were allowed to rest in air at room temperature for 1 week. Then devices were divided into four groups (2 channels in each) based on treatment: 1) native untreated PDMS, 2) oxidized PDMS stored dry, 3) oxidized PDMS stored wet, and 4) freshly oxidized PDMS. Oxidation was accomplished in a low pressure air-filled plasma oven (PDC-32G, Harrick Co.) for 30 seconds on "High" power setting (18W delivered to the RF [radio frequency] coils), and PDMS channels were bonded to a flat piece of PDMS to seal them. Groups 1 and 2 were stored dry, while group 3 channels were loaded with DI water and the whole device subsequently stored under water. After 1 week of storage under specified conditions for groups 1-3, channels from the 4th group were freshly oxidized and bonded. Then the channels from all four groups were loaded with 100 μM solution of Rhodamine B (MW=479.02 g/mole) in DI water. To minimize evaporative effects, access ports were sealed with Scotch tape and devices were stored in 100% humidity for 24 hours. After the incubation period, channels were then emptied and washed with 3 mL of DI water each. After drying with nitrogen gas, devices were sectioned and examined on an Axiovert 25 fluorescent microscope equipped with a Q-Color 5 CCD camera and TxRed fluorescent filter set. Line profiles were collected and analyzed with ImageJ.

COMSOL modeling. Simplified 2D and 3D models of the TTB were created in COMSOL Multiphysics environment (Supplemental Figure S3) to estimate diffusive fluxes of delivered agents (*i.e.,* nutrients, growth factor, and pharmaceutical treatments) and their evolution over time inside the cell culture chamber. The 2D model consisted of a 1 mm × 3 mm

rectangle representing a cross-sectional view of the cell chamber in its widest part, with eight 100 μm ×100 μm rectangles centered on top of the cell chamber simulating a cross-sectional view of the supply network. Since the fluid in the supply channels during our experiments was always moving, the concentration of the "drug" inside the modeled supply channels was assumed to be constant. For model simplicity, the supply concentration was kept at an arbitrary unit of one, while concentration inside the cell chamber was initially zero. Delivered treatment inside the supply channels was allowed to freely diffuse through the filter into the collagen-filled cell chamber with the diffusion coefficient of $D = 2.75\times10^{-12}$ m^2/s. This diffusion coefficient is for the diffusion of a ~2 MDa FITC-labeled dextran molecule inside collagen(23), representing the worst case scenario for delivery of a large molecule agent as compared to the more rapid diffusion of smaller-sized molecules, such as growth factors, antibodies, or chemical inhibitors that might be applied inside our thick-tissue bioreactor.

In the 3D model, the cell chamber was represented by a short cylinder 1 mm tall and 3 mm in diameter. Since the concentration inside the supply network channels was assumed to be constant, and in order to simplify computations and the consequent visualization, in the 3D model these channels were substituted with eight simple 100 μm wide planes acting as constant concentration boundaries positioned on top of the culture chamber. As in the case of the 2D model, the diffusion coefficient inside the chamber was assumed to be 2.75×10^{-12} m^2/s. This allowed us to visualize possible spatial perturbations of the delivered concentration gradient due to the cylindrical nature of the chamber coupled with eight rectangular channels.

Results

Effect of flow rates within the TTB. We tested several configurations of the output manifold for their ability to regulate microfluidic flow rates within the TTB, including flow channel height variation and incorporation of valves (see Figure 2 and Supplemental Figure S2). Commercial manifolds yielded a media flow rate much above the target rate of 1 ml/day (Supplemental Figure S2A). We examined whether the simple screwdriver-adjusted TURN valves could regulate media flow and drug delivery under dynamic conditions when cell population is constantly changing ((9); Supplemental Figure S2B). These valves worked extremely well for starting and stopping the flows; however, regulation of the flow through each of the individual manifold outputs using TURN valves proved to be challenging. When we used gravity-induced flow going through the input manifold to the bioreactor cartridge, any adjustments with a single TURN valve in each individual leg of the manifold splitter resulted in the flow redistribution through other reactors in the cartridge, making it difficult to accurately adjust flow through each of the individual reactors within the cartridge. As an alternative to individual channel TURN valve-adjusted flow regulators, we investigated use of pre-fabricated microfluidic flow resistance manifolds (Figure 2). Flow rates as a function of the waste manifold channel height (*i.e.*, flow resistance) were measured with the NanoFlow flow meter (IDEX Health & Science, formerly Upchurch Scientific; Figure 2B). We found that by selecting a manifold with an appropriate channel height, we could produce a sufficient resistance to flow that, in combination with the fixed height of the supply reservoir, could be used to passively limit the flow through the bioreactor (Figure 2C). This technique has proved to be quite adequate and more economical in terms of fabrication time and complexity than the TURN valve based

method. We found that 20 μm channel heights of the output manifold, while maintaining the same 100 μm width, provided the total target media flow rate of 1 mL/day.

Surface treatments of PDMS addressing possible loss of reagents/nutrients. To address concerns that some molecules could be absorbed into the PDMS surface of the cell culture chamber and thus potentially alter the actual concentration of chemicals delivered into the cell culture chamber or released by the cells during 3-week-long periods, we performed a series of experiments that used the water soluble Rhodamine B dye, which readily partitions into PDMS, as a tool to investigate methods of making the walls of PDMS microfluidic structures less likely to absorb bioreactor molecules. These experiments focused on various common surface treatments which can be easily applied to PDMS microchannels. As shown in Supplemental Figure S4, in the absence of any oxygen plasma treatments, Rhodamine easily partitions into PDMS and diffuses into the bulk of the material(22), while plasma treatment creates a silica barrier that significantly impedes such a behavior. We observed a 4-fold reduction in the amount of Rhodamine able to partition into bulk PDMS after fresh plasma oxidation of microfluidic channels. This plasma oxidation-produced barrier remains effective even after week-long storage under wet conditions (simulating a TTB reactor loaded with liquid at all times), as evidenced by the fact that these wet-stored devices maintain the same 4-fold reduction in Rhodamine partitioned into the bulk. Thus, plasma treatment of PDMS surfaces facilitates not only wetability and loading of the TTB but also produces a barrier impeding chemical partitioning and loss during long-term culture conditions.

TTB supports long-term organotypic growth. The ability of the TTB to sustain growth of organotypic cultures over extended periods of time was demonstrated using the MCF-10A cell line and its invasive and tumorigenic variants. Long-term culture of the MCF-10A cell line

within 3D Matrigel follows a morphogenic program that results in a mammosphere structure with a hollow lumen over the course of 3 weeks. Mammosphere morphogenesis can be visualized in our closed bioreactor system using a live cell stain to visualize nuclei combined with confocal microscopy. The TTB slide and clamp system were purposefully designed to allow placement into standard microscopy systems and, considering the short working distances of confocal microscopy, to allow real-time *in situ* imaging of the cellular processes at different times during mammosphere growth. The TTB cell chamber depth was standardized to the ECM gel depth of the organotypic culture system that we utilized. Furthermore, the MCF-10A variants have varying irregular features that are readily visualized in the closed TTB system. A series of confocal images for MCF-10A, MCF-10AT1, and MCF-10CA1d variants is shown in Figure 3. These mammospheres have successfully matured from individual cells within the TTB over a period of 21 days. The complete stack of confocal images is shown in Supplemental Figure S5.

Drug delivery within the TTB system. As a first step towards validation of drug delivery in our TTB, we applied increasing concentrations of a commonly used chemotherapeutic, docetaxel, for 24 hours to MCF CA1d cells within the TTB and a traditional 8-well culture chamber(24;25). Docetaxel treatment resulted in a dose-dependent increase in cell death of MCF-10 CA1d cells in both systems at concentrations that are commonly toxic to a wide range of cells ((26;27)Supplemental Figure S6). For the next step, as we were interested in monitoring cellular changes within a 3D organotypic microenvironment of a long-term cell culture system, we evaluated the ability of a known inhibitor to blunt cellular growth in our reactor system and compared results with our side-by-side tests using traditional cell culture techniques. Mammosphere formation is dependent upon a number of cellular processes and is regulated by extracellular proteinase activity. A matrix proteinase inhibitor cocktail known to

target a broad spectrum of extracellular matrix proteinase activity was used (Aprotinin, for serine; GM6001, for metallo-; E-64, for cysteine; and Pepstain A, for aspartic; Calbiochem)(28). As we wanted to demonstrate long-term delivery of drug into our system, we first determined the amount of drug that could be continuously added to traditional cell culture without affecting long-term cell viability. For these experiments, we applied the matrix proteinase inhibitor cocktail to monolayer cell cultures in incrementally higher concentrations and evaluated cell viability using the Live/Dead Assay (Molecular Probes). High concentration ranges of the proteinase inhibitor cocktail that have proven effective to inhibit cellular processes such as cellular migration are toxic to cells with 48 hours of continuous application (28); however, the concentration we chose for long-term drug delivery evaluation within the TTB system did not have an impact on cell viability (see Supplemental Figure S7) yet retained its inhibitory properties.

Next, we assessed whether this non-toxic concentration of proteinase inhibitor cocktail was still effective as an extracellular matrix inhibitor within organotypic cell cultures. First, mammosphere formation of MCF-10A cells achieved with the traditional cell culture methods was blunted with addition of this non-toxic proteinase inhibitor cocktail (Figure 4A). Second, we measured proteinase inhibition of proteinase activity in developing organotypic cultures within the TTB. For these experiments, we used the overlay method for establishing 6-day-old mammospheres. Additionally, because it is known that reduced growth factor Matrigel contains trace matrix proteinase content, and because we wanted to improve the baseline sensitivity of the proteinase activity assay, we cultured the MCF-10A cells and variants in a Matrigel:hydrogel mixture. The defined artificial matrix (*i.e.,* hydrogel) contains low endogenous proteolytic activity that allowed for visualization of cell-associated proteolytic activity. The 1:1 mixture did

not affect long-term mammosphere formation within the time frame evaluated. Following 6 days of culture, mammospheres were overlaid with hydrogel containing fluorogenic probe (DQ-gelatin). The mammospheres were cultured in the presence and absence of matrix proteinase inhibitor cocktail for 48 hours. As shown in Figure 4B, MCF-10AT1 organotypic cultures demonstrated robust proteinase activity, as indicated by the increase of fluorescein fluorescence of the matrix-embedded DQ-gelatin. However, there was a notable reduction in proteinase activity surrounding mammospheres cultured in the presence of proteinase inhibitors. Our results demonstrate effective protease inhibition using these concentrations of the proteinase inhibitor cocktail.

We next evaluated long-term drug delivery within the TTB. Using organotypic cultures of the MCF-10A human mammary epithelial cell line and their invasive counterparts grown within the TTB, we assessed mammosphere formation in the absence and presence of continuous application of the protease inhibitor cocktail that targets a broad spectrum of extracellular matrix proteinase activity into the system. As shown in Figure 5, this protease inhibitor cocktail down-regulated morphogenesis of the MCF-10A variants within the TTB. MCF-10A cell lines showed on average a ~32% reduction in mammosphere diameter, whereas the MCF-10 -AT, -CA1a, and -CA1d demonstrated a more robust average reduction in mammosphere diameter of ~ 73%, 61%, and 67%, respectively. Interestingly, the sensitivity of the proteinase inhibitory effects correlates well with endogenous matrix proteinase activity of these cell lines. Conditioned media collected from MCF-10A and MCF-10 -AT, -CA1a, and -CA1d grown under 2D monolayer culture conditions was compared for its ability to cleave denatured collagen (*i.e.,* DQ-gelatin). MCF-10A had the lowest measureable endogenous matrix proteinase degrading ability at a rate of 112.2 ± 22.4 (AU/min± SE). MCF-10 -AT, -CA1a, and -CA1d cell line variants had higher rates

of measured degradation ability at 168.2±18.8, 123.2±27.8, and 169.7±31.3 (AU/min± SE). Since the endogenous proteinase activity for MCF-10A is less when compared to its tumorigenic variants, it would be logical to expect that the decrease in mammosphere size would also be the least out of the whole cell panel. Overall, these results suggest that *in vitro* acinar development and the subsequent down-regulation of mammosphere formation were correlated with pharmacological down-regulation of matrix proteinase activity in these cell systems. Additionally, our results are supported by a short, 5-day 3D static culture of T47D breast carcinoma cells in collagen inside a microfluidic channel (15), where a 45% decrease in the size of cell clusters formed was observed after the incubation with a single MMP inhibitor GM6001. In general, our studies demonstrate the utility of the TTB for long-term organotypic culture and continuous drug delivery within a closed system with capabilities for optical analysis of cellular functions.

Conclusions

We have developed a portable thick-tissue bioreactor (TTB) capable of maintaining sterile microenvironment and sustaining cell growth, maturation, and organ formation during 3 week-long cell culture. The performance of the TTB was validated with the MCF-10A cell line and its invasive and tumorigenic variants that were capable of developing into hollow lumen spheroids when cultured in 3D matrix over the course of 21 days. Real-time staining and visualization of fully developed mammospheres were possible within the closed bioreactor system. The fully assembled TTB was compatible with regular and fluorescent microscopy and allowed optical assessment of the mammosphere development and proteinase activity using confocal microscopy. The potential drug delivery into our bioreactor system to monitor changes

in cellular functions was demonstrated by reduction of mammosphere formation upon delivery of matrix proteinase inhibitors into the closed bioreactor system, as well as in overall reduction of proteinase activity. We created both 2D and 3D COMSOL models to estimate drug delivery and gradient evolution into the cell culture chamber of the bioreactor. The TTB would be readily amenable to other organotypic cell systems. Due to the small cell chamber volumes, it would be particularly useful in systems that utilize cells that are difficult to obtain, such as primary cells, stem cells, or patient tumor cell lines, or in experiments where the cellular secretions need to be analyzed with minimal dilution(29;30). It would be beneficial as a high-throughput microfluidic device compatible with 3D organotypic cell culture that would allow testing of various treatment options to select the one of optimal benefit to the patient. Finally, we demonstrated that microfluidic channels separated by a porous membrane from a small chamber filled with collagen can provide long-term perifusion of cells actively growing in a three-dimensional matrix.

ACKNOWLEDGMENTS

This research was supported by the Department of Defense Breast Cancer Research Program (DOD BCRP) grants W81XWH-09-1-0444 and W81XWH-10-1-0157 to L.J.M. and W81XWH-07-1-0507 to J.P.W.; by the National Institutes of Health grant U54CA113007; and by the Vanderbilt Institute for Integrative Biosystems Research and Education (VIIBRE). We thank David Shifrin and John Huidekoper for technical assistance, and Allison Price and Don Berry for editorial assistance.

Figure Legends

Figure 1. Design of the Thick Tissue Bioreactor (TTB). A) A photograph of the TTB filled with blue and red dyes indicating microfluidic supply network (blue) and the cell culture chambers (red) beneath the perifusion channels; B) A close view of the binary flow divider with ceiling support pillars and a cell culture chamber; C) Block diagram of the typical layout for the clamped TTB indicating major components; D) A photograph of the clamped TTB cartridge with a schematic diagram illustrating the set-up for long-term culture; E) A photograph of the fully assembled TTB prototype with the gravity-driven feeding system, passively regulated flow through the input/output manifold, and a Labtainer™ from HyClone as a waste containment system.

Figure 2. Effect of the channel heights within the output manifold on the total flow rate through the TTB. A) A block diagram of the experimental set-up. B) Typical flow rates through the TTB with the output manifolds of 100 μm channel widths and varying channel heights. C) Flow rate as a function of output manifold channel height. Each point is a 20-minute average with error bars (covered by the dots) representing standard deviations with the corresponding LOD = 0.35 nl/min. D) A photograph of the TTB connected to the input and output manifolds.

Figure 3. Selected confocal slices of MCF cell variants cultured within the TTB for 21 days. Mammospheres formed by MCF-10A, MCF-10AT1, and MCF-10CA1d cells labeled with Alexa 488 phalloidin (Green, which is an actin stain) and with SYTO-63 (Red, a nuclear stain for the live cells). (10X). Note the hollow lumens formed by the MCF-10A in contrast to the filled, grape-like cell clusters typical of the tumorigenic MCF-10 CA1d cell line.

Figure 4. Proteinase inhibitor delivery into the TTB. (A) Matrix proteinase inhibitor (PI) treatments of organotypic culture of MCF-10A cell variants (+) shows a reduction in

mammosphere size as compared to control (-). (B) Inhibition of proteinase activity was confirmed by confocal microscopy of MCF-10A cell variants that were grown for 5 days within TTB and then overlaid with matrix containing fluorogenic protease activity probe (25 μg/ml DQ-gelatin in hydrogel). Following 48 hours, protease activity was detected by an increase in fluorescence due to proteolysis of DQ-gelatin (Ex/Em 495/515 nm; Molecular Probes). Images representative of one plane of a z-stack (40x).

Figure 5. Results for the proteinase inhibitor treatment of various MCF-10A and cell line variants. Cells cultured within the TTB for 21 days and exposed to PI treatment demonstrate reduction in the size of the formed mammospheres (+) as compared to control (-). The protease inhibitor cocktail is defined in "Methods." Images were taken *in situ* with the TTB being fully assembled and continuously perifused, as shown in Figure 1D.

Supplemental Figure Legends

Supplemental Figure S1. Visual representation of the TTB components going through two sterilization procedures. Cell chambers with stainless steel clamps are autoclaved and the rest of the components are pre-assembled in clean environment and sterilized by gamma irradiation.

Supplemental Figure S2. Different manifold configurations tested. Additional splitter configurations tested. A) Four-way manifolds from Small Parts, Inc. and B) Microfluidic manifolds with built-in TURN valves.

Supplemental Figure S3. Simplified 2D and 3D diffusional model illustrating time course of the "drug" diffusion into the TTB chamber filled with collagen. The perifusion supply

channels (dark squares) are 100 by 100 μm, the culture chamber (blue rectangle) is 1 mm by 3 mm, and a large molecule "drug" with a diffusion coefficient D = $2.75e^{-12}$ m^2/s, which is equivalent for the measured diffusion coefficient of the ~2 MDa FITC-labeled dextran through collagen. The false color indicates concentration (1 being 100% of the initial concentration delivered into the system), and the lower right figure shows the spatial distribution of iso-concentration surfaces within the collagen.

Supplemental Figure S4. Partition of Rhodamine B into PDMS as a function of surface treatments. A) The observed fluorescence of the Rhodamine B diffused into PDMS through the walls of the 50 μm by 50 μm channel. B) Line profiles of the fluorescence intensity extending from the channel ceiling into PDMS bulk.

Supplemental Figure S5. Confocal slices of MCF cell variants cultured within the TTB for 21 days. Mammospheres formed by (A) MCF-10A, (B) MCF-10AT1, and (C) MCF-10CA1d cells labeled with Alexa 488 phalloidin (green, which is an actin stain) and with SYTO-63 (red, a nuclear stain for the live cells). (10X). Note the hollow lumens formed by the MCF-10A in contrast to the filled, grape-like cell clusters typical of the tumorigenic MCF-10 CA1d cell line.

Supplemental Figure S6. Dose-dependent toxicity to increasing amounts of docetaxel affecting viability as evaluated by Live-Dead Viability Assay.MCF-10 CA1d cells were cultured in (A) a cell culture chamber or (B) the TTB in the absence (-) or in the presence of docetaxel (0, 10, 100, 1000 ng/ml). Following 24-hour incubation with docetaxel, the dose-dependent effect of docetaxel on cellular viability was evaluated by Live-Dead Viability Assay.

Data are expressed as the ratio of Live (Calcein AM accumulation) to Dead (Ethidium) fluorescence staining. Data are expressed as Average Ratio ±SE (n=4).

Supplemental Figure S7. Dosage-dependent proteinase inhibitor cocktail toxicity effects on MCF-10A and MCF-10CA1d cells. MCF-10A and -10 CA1d cells were cultured in the absence (-) or in the presence of combination proteinase inhibitor cocktail at three doses (2x, 1x, and 0.2x). Dose-dependent toxicity to increasing amounts of proteinase inhibitor treatment affecting viability was evaluated by Live-Dead Viability Assay at 1μM of Calcein AM (green=live) and 2μM of Ethidium homodimer-1 (red=dead). Inhibitor treatment in Figures 4 and 5 used a drug concentration that was chosen to be non-toxic to cells.

Reference List

1. Bissell MJ, Radisky D. Putting tumours in context. Nat Rev Cancer 2001;1:46-54

2. Schmeichel KL, Bissell MJ. Modeling tissue-specific signaling and organ function in three dimensions. J.Cell Sci. 2003 Jun 15;116(Pt 12):2377-88

3. Debnath J, Brugge JS. Modelling glandular epithelial cancers in three-dimensional cultures. Nat.Rev.Cancer 2005 Sep;5(9):675-88

4. Nicholson KM, Bibby MC, Phillips RM. Influence of drug exposure parameters on the activity of paclitaxel in multicellular spheroids. Eur.J Cancer 1997 Jul;33(8):1291-8

5. Wu MH, Huang SB, Cui ZF, Cui Z, Lee GB. Development of perfusion-based micro 3-D cell culture platform and its application for high throughput drug testing. Sensors and Actuators B-Chemical 2008 Jan 29;129(1):231-40

6. Debnath J, Muthuswamy SK, Brugge JS. Morphogenesis and oncogenesis of MCF-10A mammary epithelial acini grown in three-dimensional basement membrane cultures. Methods 2003 Jul;30(3):256-68

7. Griffith LG, Swartz MA. Capturing complex 3D tissue physiology in vitro. Nature Rev.Mol.Cell Biol. 2006;7(3):211-24

8. Wikswo JP, Prokop A, Baudenbacher F, Cliffel D, Csukas B, Velkovsky M. Engineering challenges of BioNEMS: the integration of microfluidics, and micro- and nanodevices, models, and external control for systems biology. IEE Proc.-Nanobiotechnol. 2006;153(4):81-101

9. Markov DA, Manuel S, Shor L, Opalenik SR, Wikswo JP, Samson PC. Tape underlayment rotary-node (TURN) valves for simple on-chip microfluidic flow control. Biomed.Microdevices 2010;12(1):135-44

10. Wu LY, Di Carlo D, Lee LP. Microfluidic self-assembly of tumor spheroids for anticancer drug discovery. Biomedical Microdevices 2008 Apr;10(2):197-202

11. Tourovskaia A, Figueroa-Masot X, Folch A. Differentiation-on-a-chip: A microfluidic platform for longterm cell culture studies. Lab Chip 2005;5:14-9

12. Tenstad E, Tourovskaia A, Folch A, Myklebost O, Rian E. Extensive adipogenic and osteogenic differentiation of patterned human mesenchymal stem cells in a microfluidic device. Lab Chip 2010;10(11):1401-9

13. Hattersley SM, Dyer CE, Greenman J, Haswell SJ. Development of a microfluidic device for the maintenance and interrogation of viable tissue biopsies. Lab Chip. 2008 Nov;8(11):1842-6

14. Dhurjati R, Liu X, Gay CV, Mastro AM, Vogler EA. Extended-Term Culture of Bone Cells in a Compartmentalized Bioreactor. Tissue Engineering 2006 Nov 30;12(11):3045-54

15. Bauer M, Su G, Beebe DJ, Friedl A. 3D microchannel co-culture: method and biological validation. Integr.Biol. 2010;2(7-8):371-8

16. Jo BH, Van Lerberghe LM, Motsegood KM, Beebe DJ. Three-dimensional micro-channel fabrication in polydimethylsiloxane (PDMS) elastomer. J.Microelectromech.S. 2000;9(1):76-81

17. Leclerc E, Sakai Y, Fujii T. Microfluidic PDMS (polydimethylsiloxane) bioreactor for large-scale culture of hepatocytes. Biotechnol.Progr. 2004;20(3):750-5

18. Santner SJ, Dawson PJ, Tait L, Soule HD, Eliason J, Mohamed AN, Wolman SR, Heppner GH, Miller FR. Malignant MCF10CA1 cell lines derived from premalignant human breast epithelial MCF10AT cells. Breast Cancer Res.Treat. 2001 Jan;65(2):101-10

19. Markov DA, Lillie EM, Samson PC, Wikswo JP, McCawley LJ. Chips & Tips: A method for periodic sterile sample collection during continuous cell culture in microfluidic devices. Lab on a Chip 2010 Aug 17; http://www.rsc.org/Publishing/Journals/lc/Chips_and_Tips/microfluidic_devices.asp

20. White JD. Standard aeration for gas-sterilized plastics. J.Hyg.(Lond) 1977 Oct;79(2):225-32. PMCID:PMC2129942

21. McIntyre JO, Fingleton B, Wells KS, Piston DW, Lynch CC, Gautam S, Matrisian LM. Development of a novel fluorogenic proteolytic beacon for in vivo detection and imaging of tumour-associated matrix metalloproteinase-7 activity. Biochem.J. 2004 Feb 1;377(Pt 3):617-28

22. Toepke MW, Beebe DJ. PDMS absorption of small molecules and consequences in microfluidic applications. Lab Chip. 2006 Dec;6(12):1484-6

23. Thorsen T, Maerkl SJ, Quake SR. Microfluidic Large-Scale Integration. Science 2002 Sep 26;298:580-4

24. Crown J, O'Leary M, Ooi WS. Docetaxel and paclitaxel in the treatment of breast cancer: a review of clinical experience. Oncologist. 2004;9 Suppl 2:24-32

25. Ward S, Simpson E, Davis S, Hind D, Rees A, Wilkinson A. Taxanes for the adjuvant treatment of early breast cancer: systematic review and economic evaluation. Health Technol.Assess. 2007 Oct;11(40):1-144

26. Hernandez-Vargas H, Palacios J, Moreno-Bueno G. Telling cells how to die: docetaxel therapy in cancer cell lines. Cell Cycle 2007 Apr 1;6(7):780-3

27. Morse DL, Gray H, Payne CM, Gillies RJ. Docetaxel induces cell death through mitotic catastrophe in human breast cancer cells. Mol.Cancer Ther. 2005 Oct;4(10):1495-504

28. Wolf K, Mazo I, Leung H, Engelke K, Von Andrian UH, Deryugina EI, Strongin AY, Brocker EB, Friedl P. Compensation mechanism in tumor cell migration: mesenchymal-amoeboid transition after blocking of pericellular proteolysis. J Cell Biol. 2003 Jan 21;160(2):267-77

29. Enders JR, Goodwin CR, Marasco CC, Seale KT, Wikswo JP, Mclean JA. Advanced structural Mass Spectrometry for Systems biology: Pulling the Needles from Haystacks. Spectroscopy Supp.Curr.Trends Mass Spectrometry 2011;July:18-23

30. Enders JR, Marasco CC, Kole A, Nguyen B, Sundarapandian S, Seale KT, Wikswo JP, Mclean JA. Towards monitoring real-time cellular response using an integrated microfluidics-MALDI/NESI-ion mobility-mass spectrometry platform. IET Syst.Biol. 2010;4(6):416-27

Figure 1

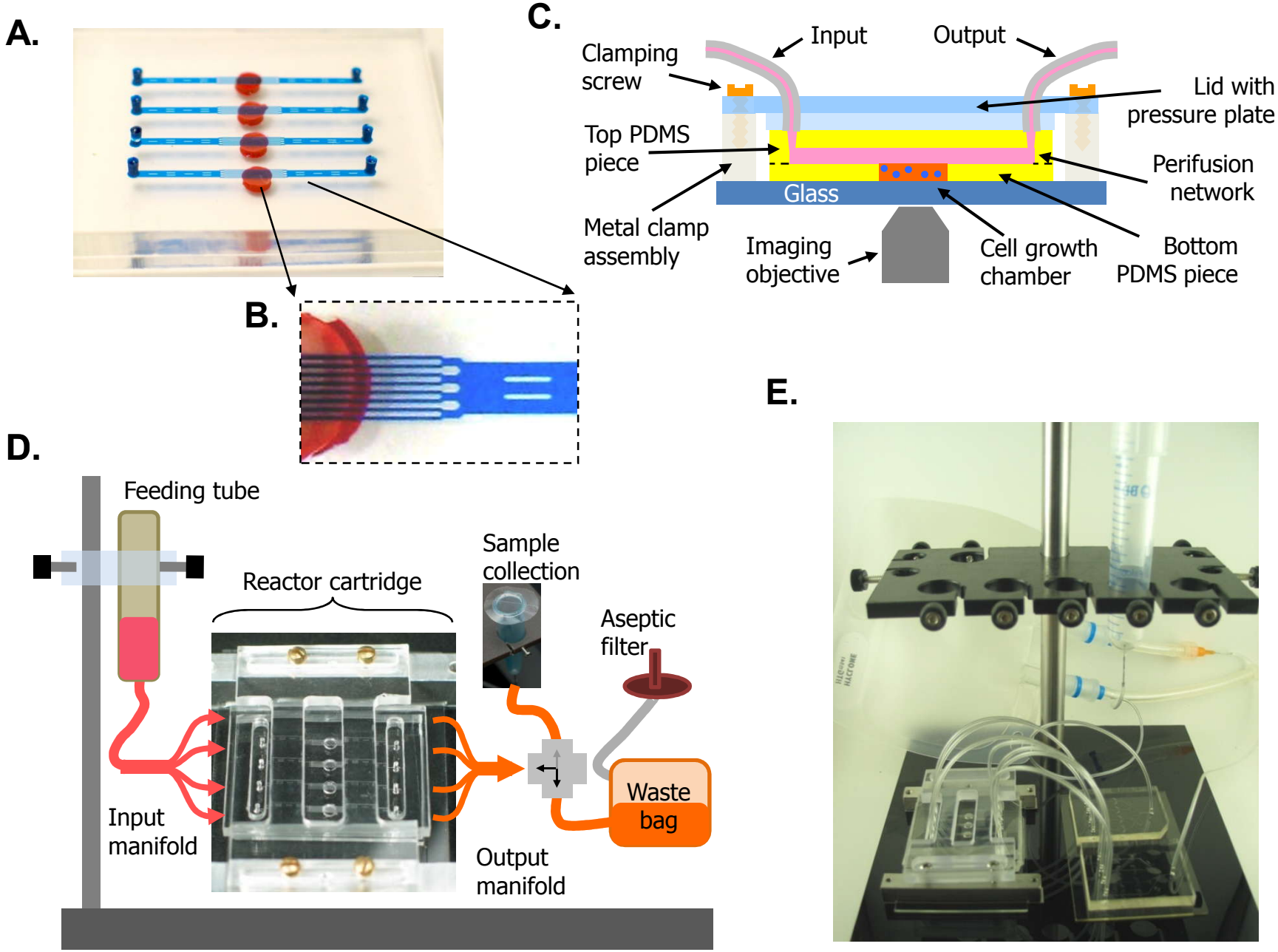

Figure 2

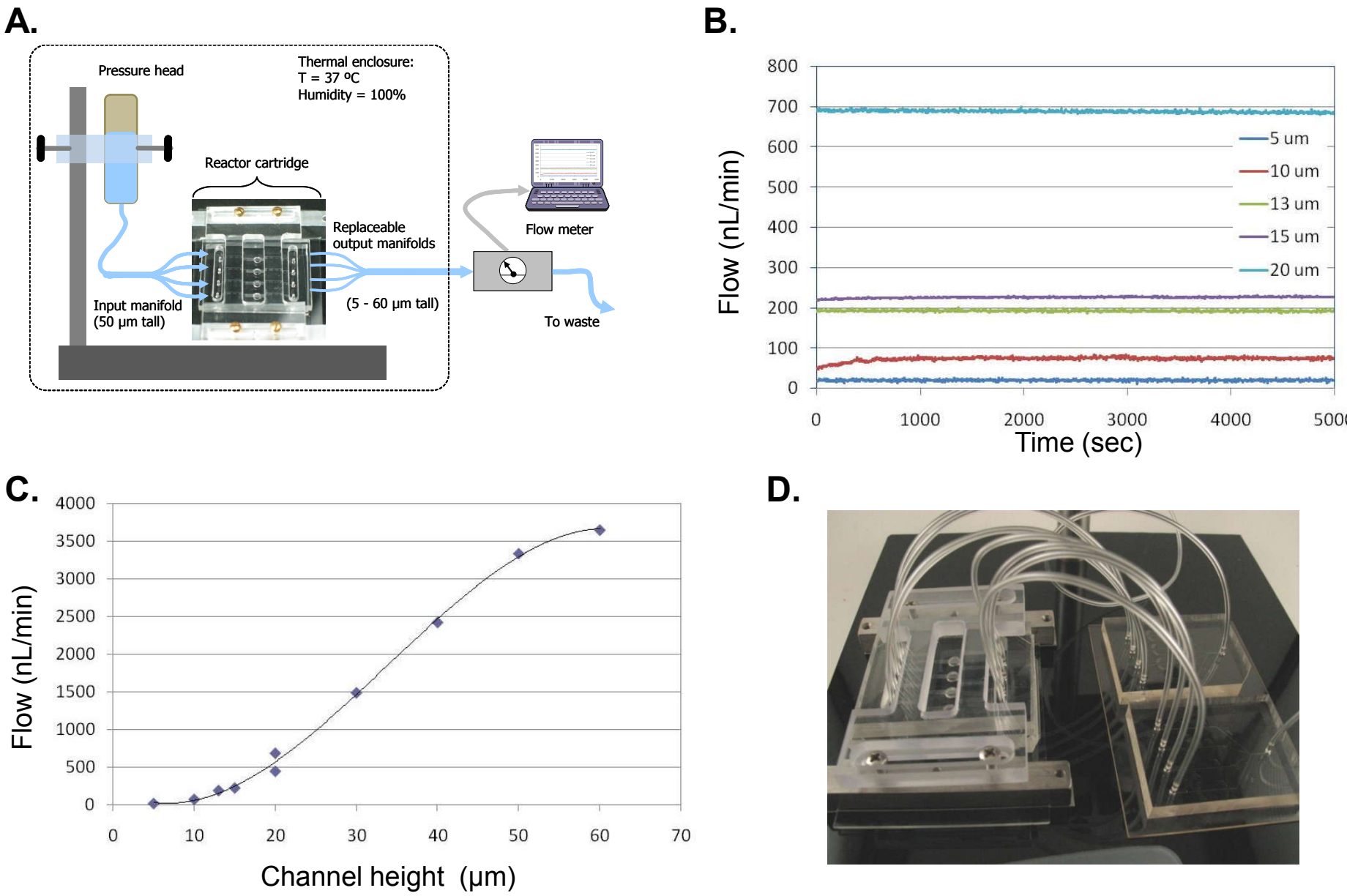

Figure 3

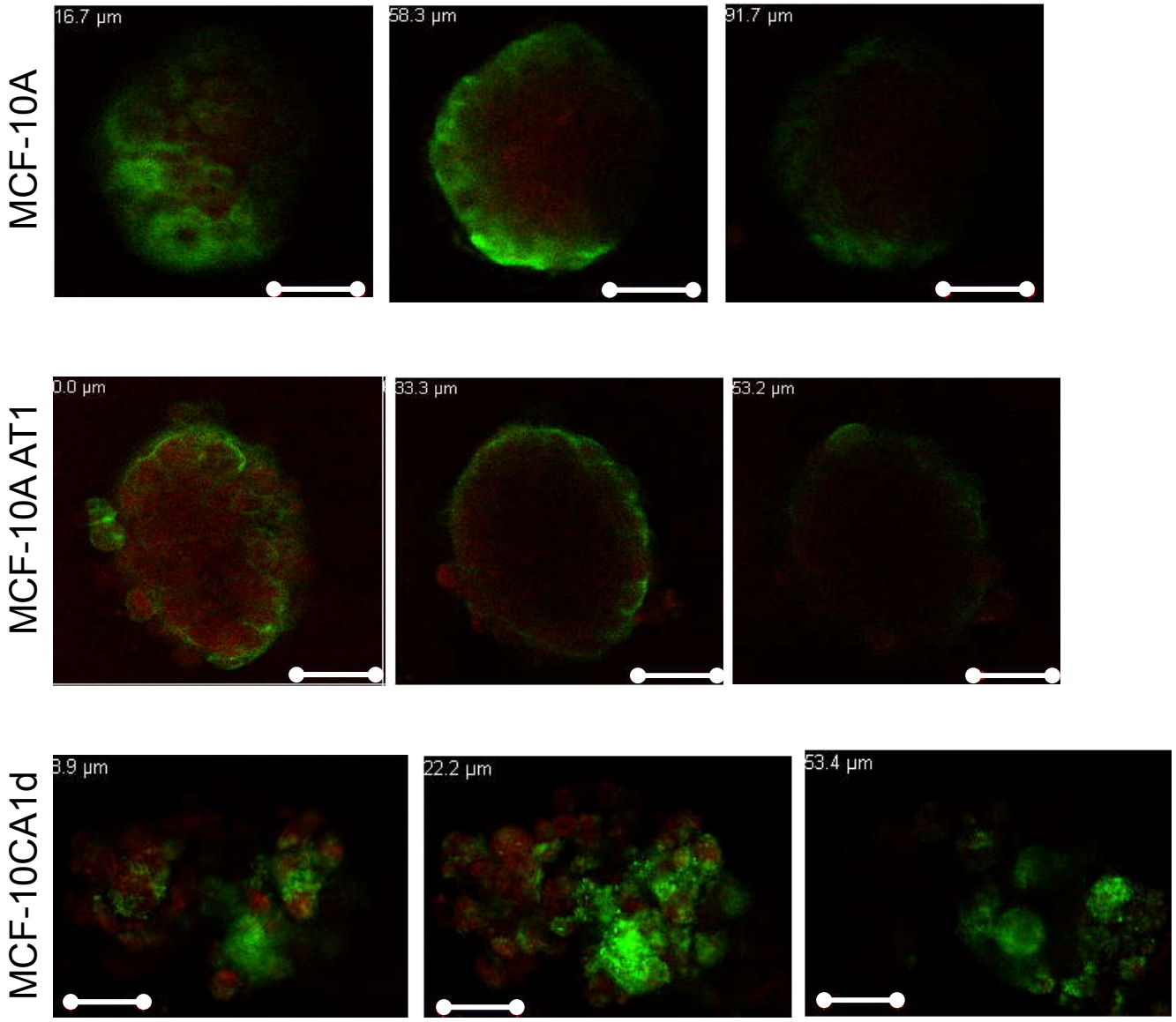

Calibration bars are 50 µm.

Figure 4

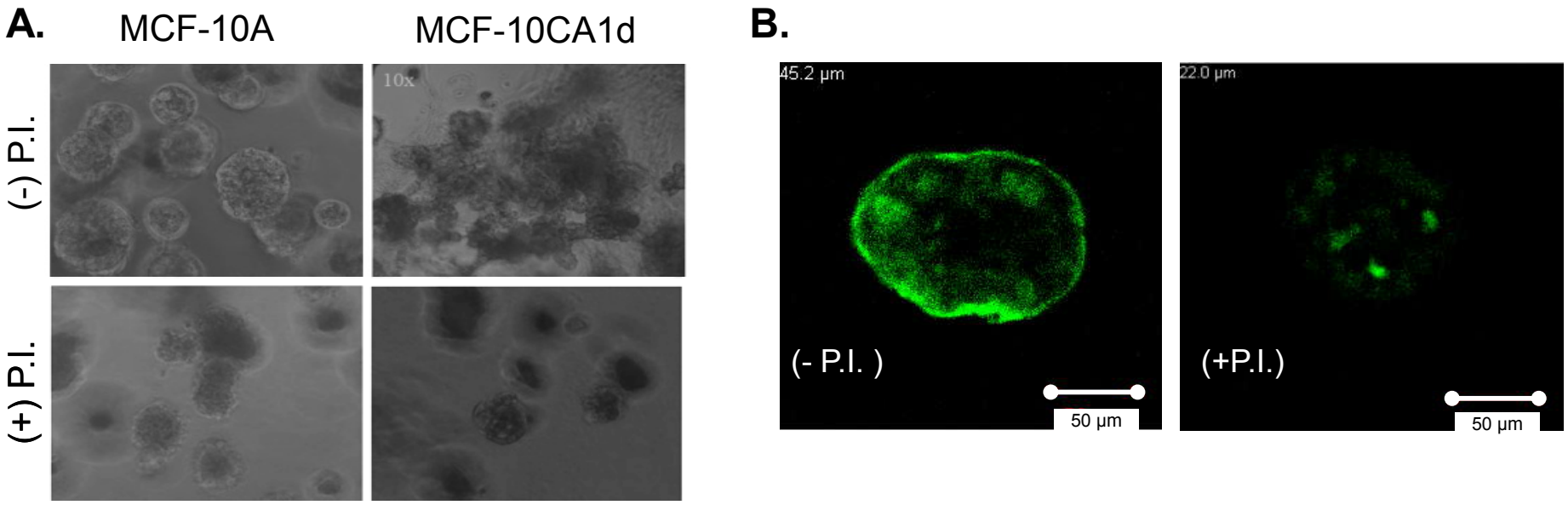

Figure 5

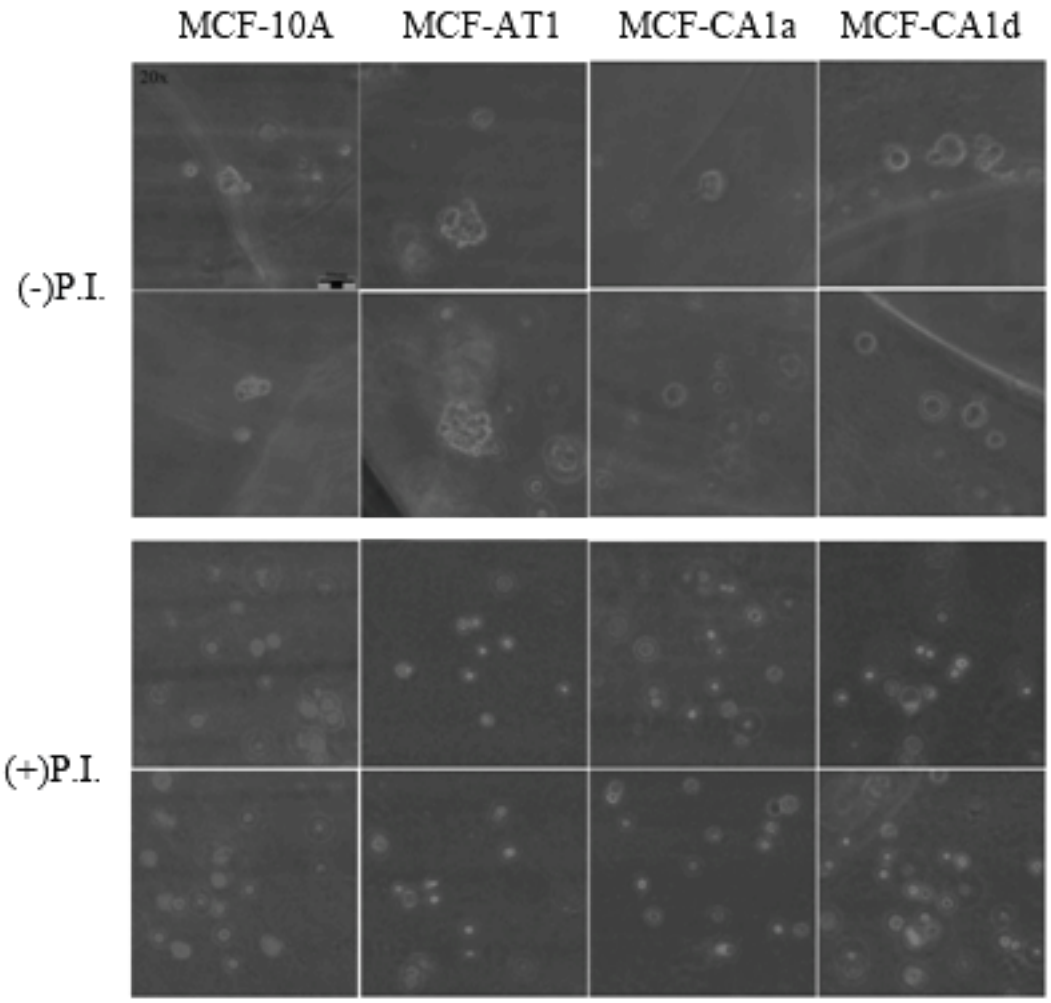

Supplemental

Supplemental Figure S1

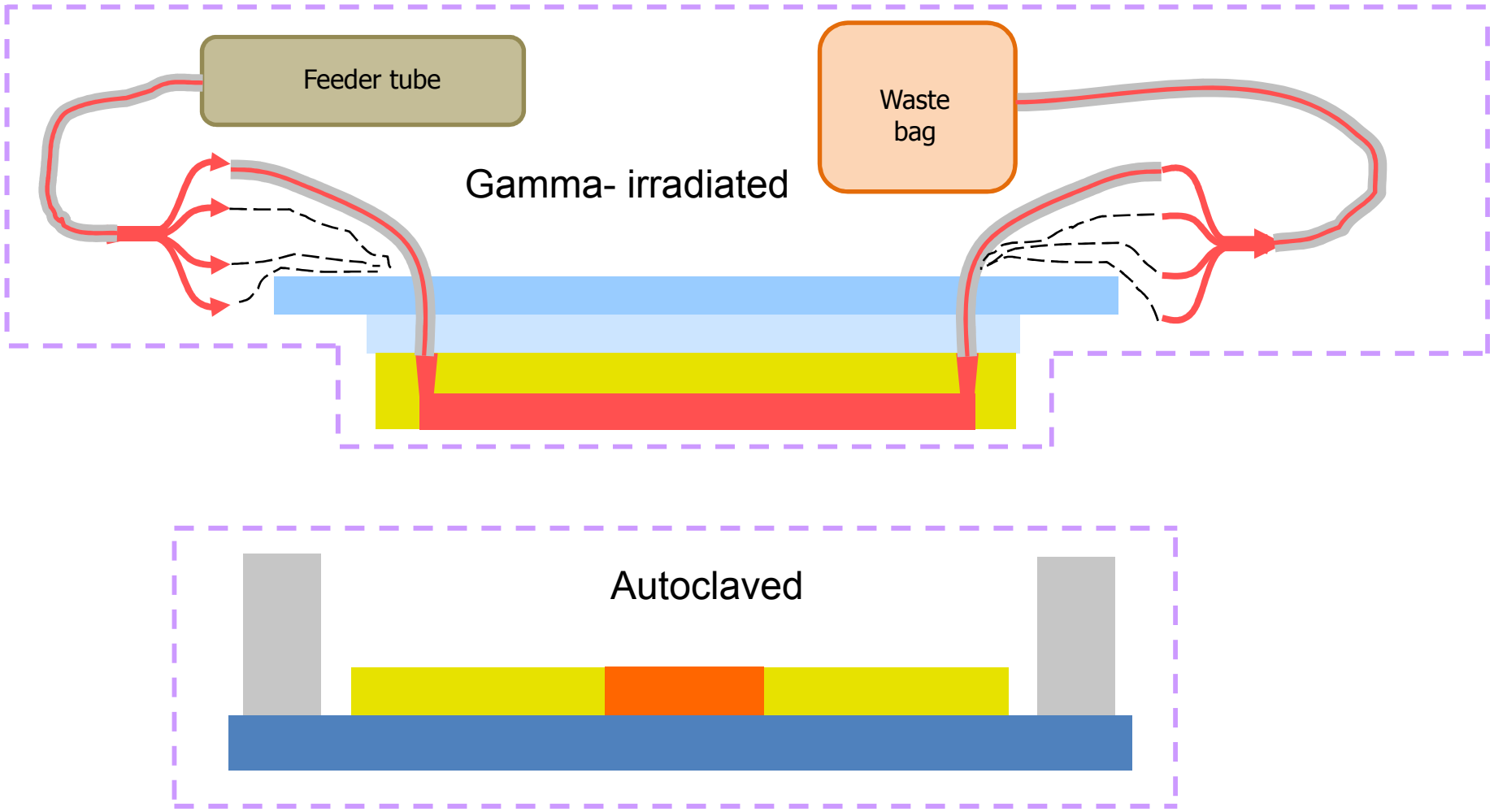

Supplemental Figure S2

A

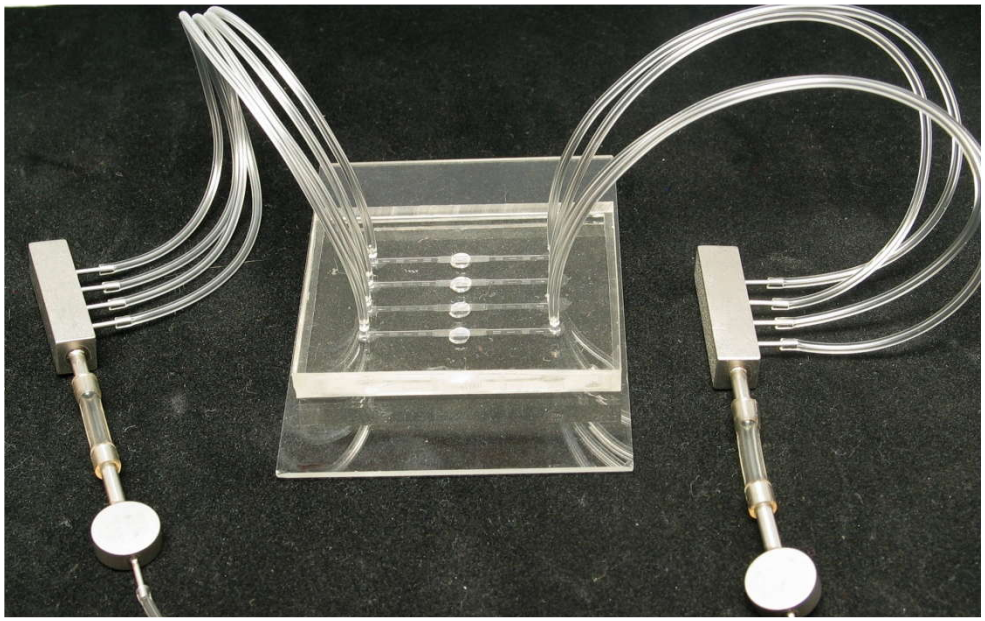

B

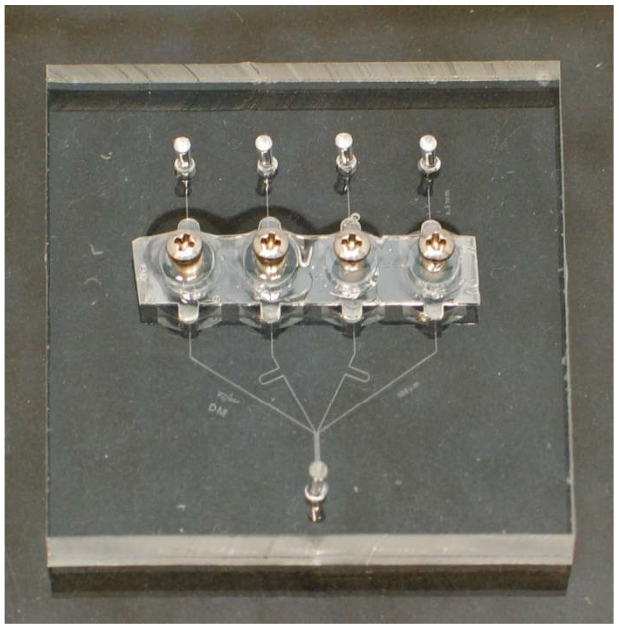

Supplemental Figure S3

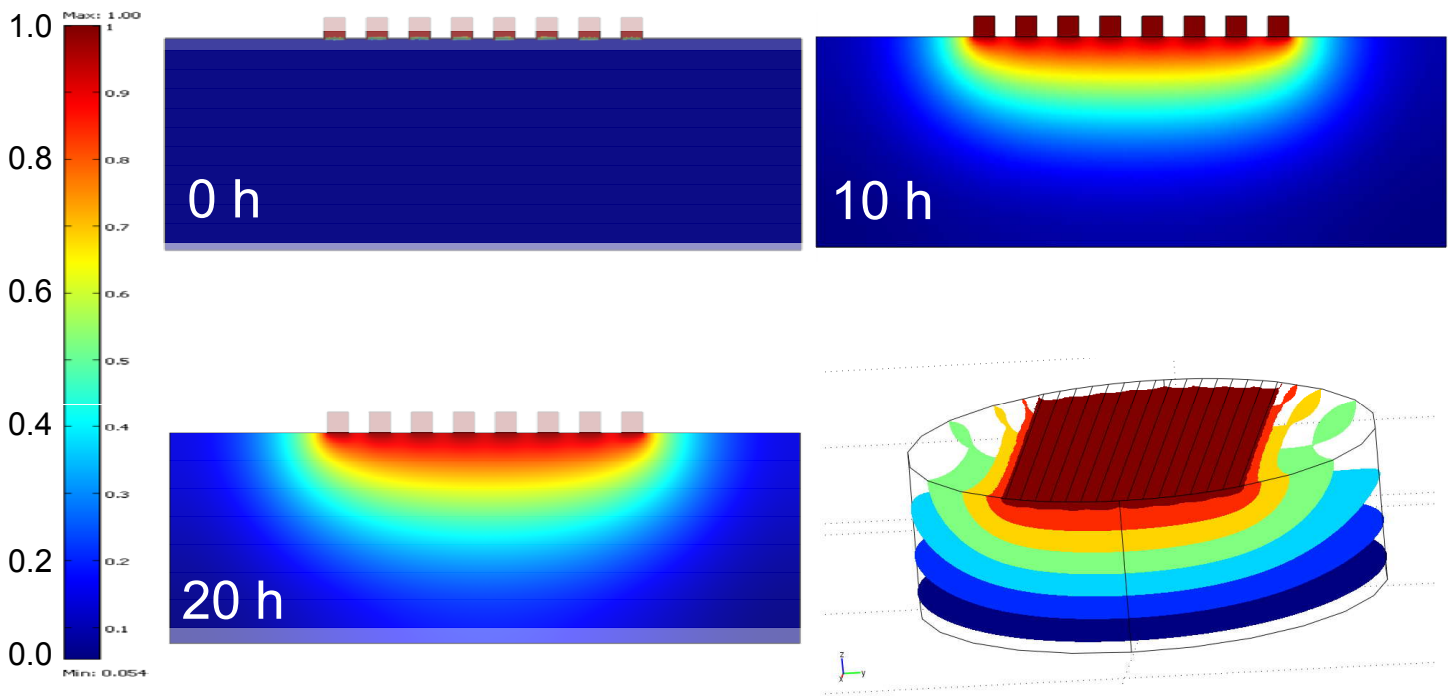

Supplemental Figure S4

A.

B.

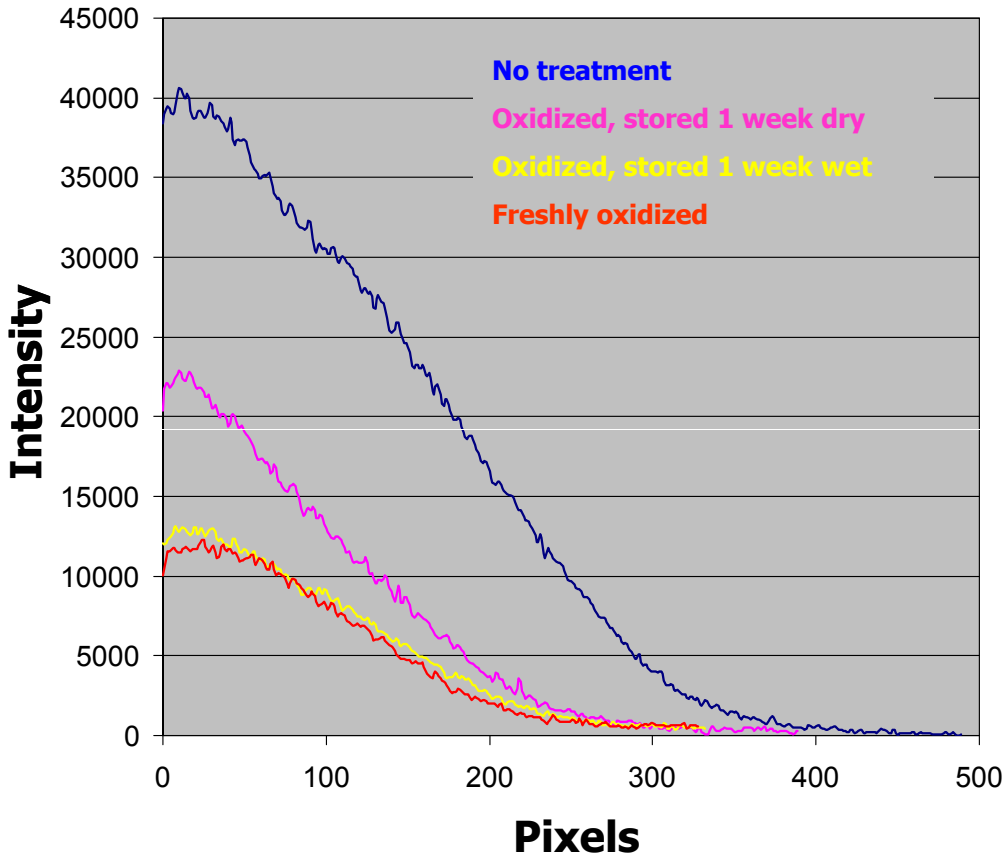

Supplemental Figure S5A

A.

MCF-10A

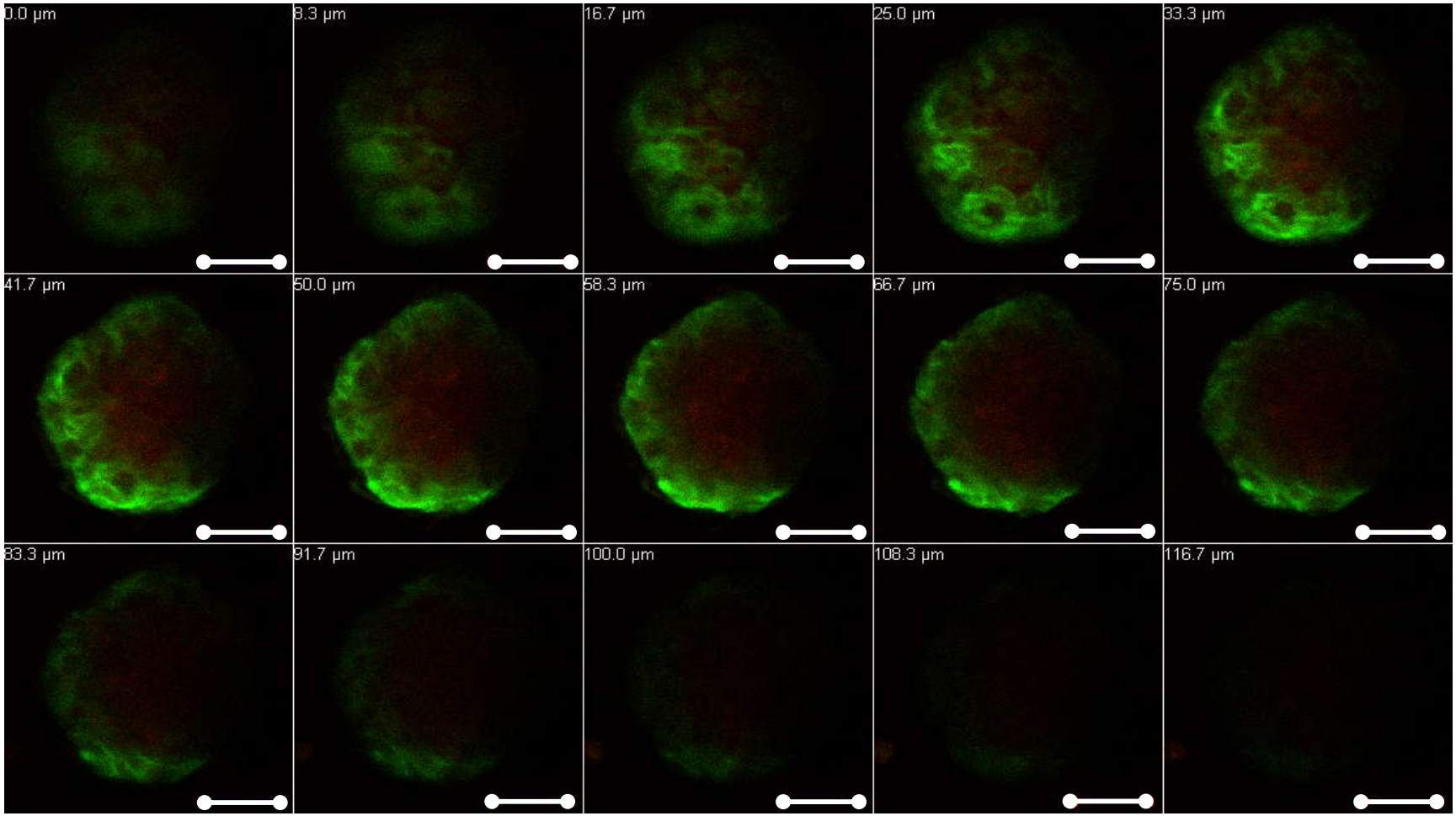

Supplemental Figure S5B

B.

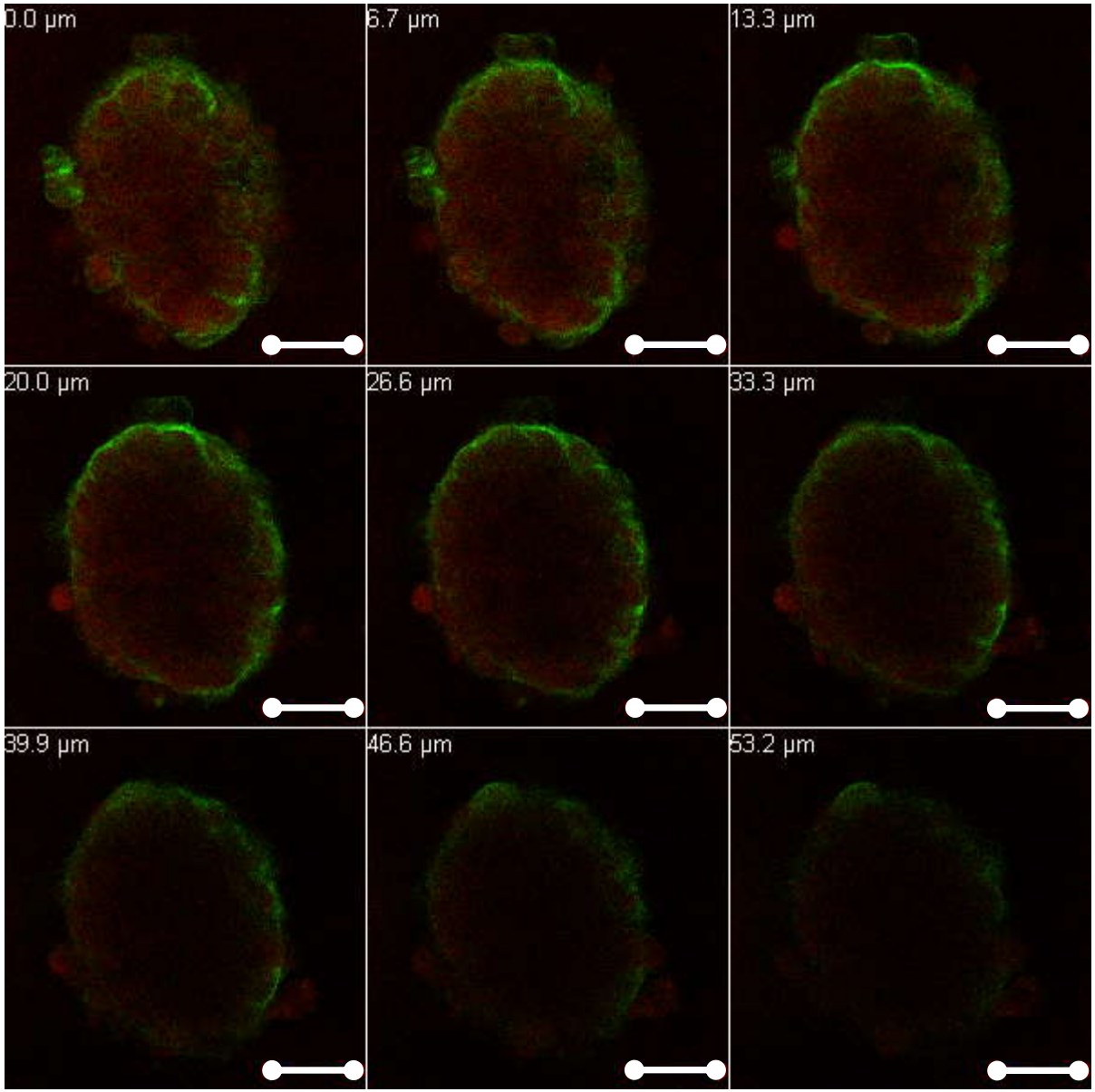

Supplemental Figure S5C

C. MCF-10 CA 1d

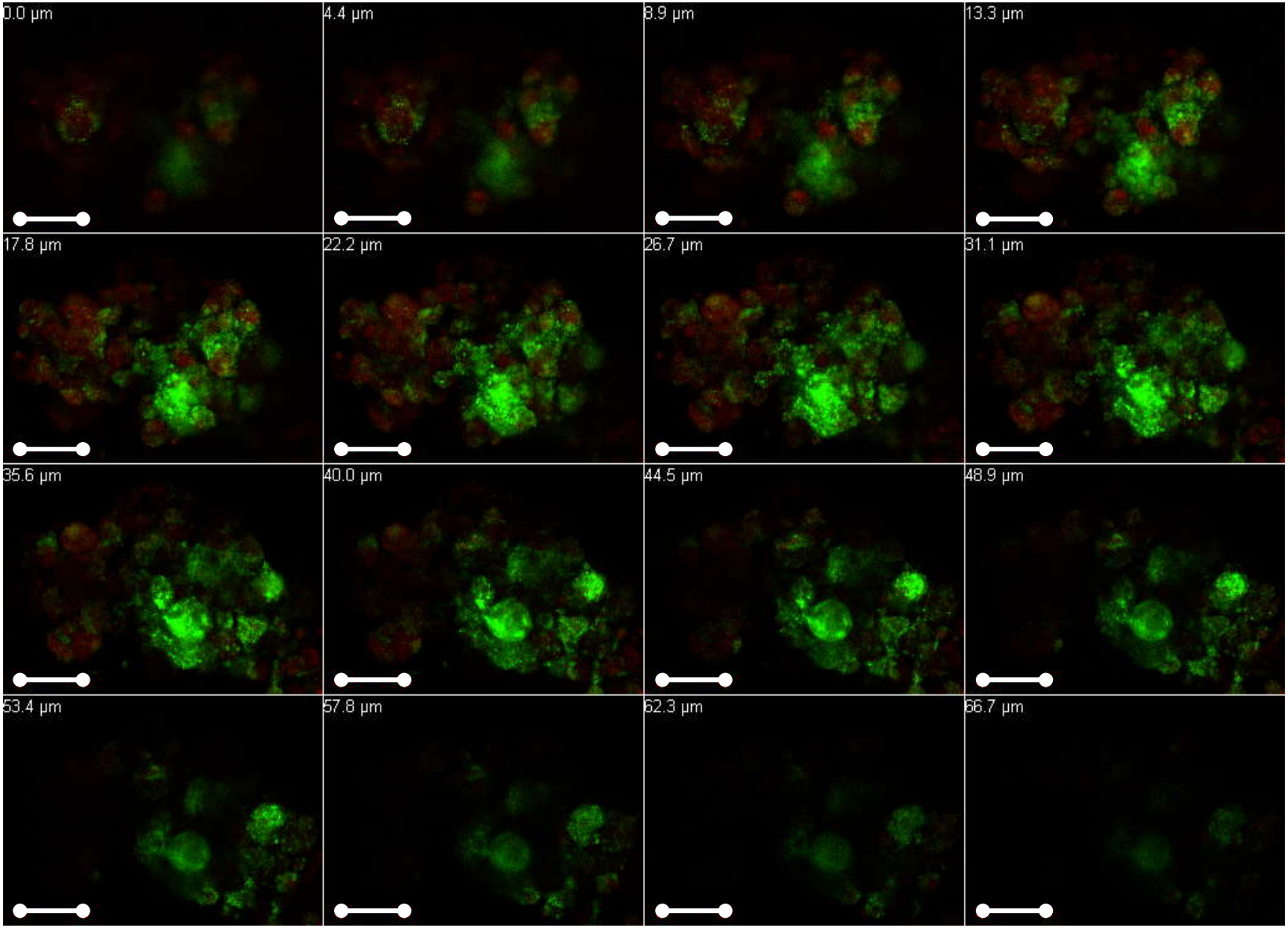

Supplemental Figure S6

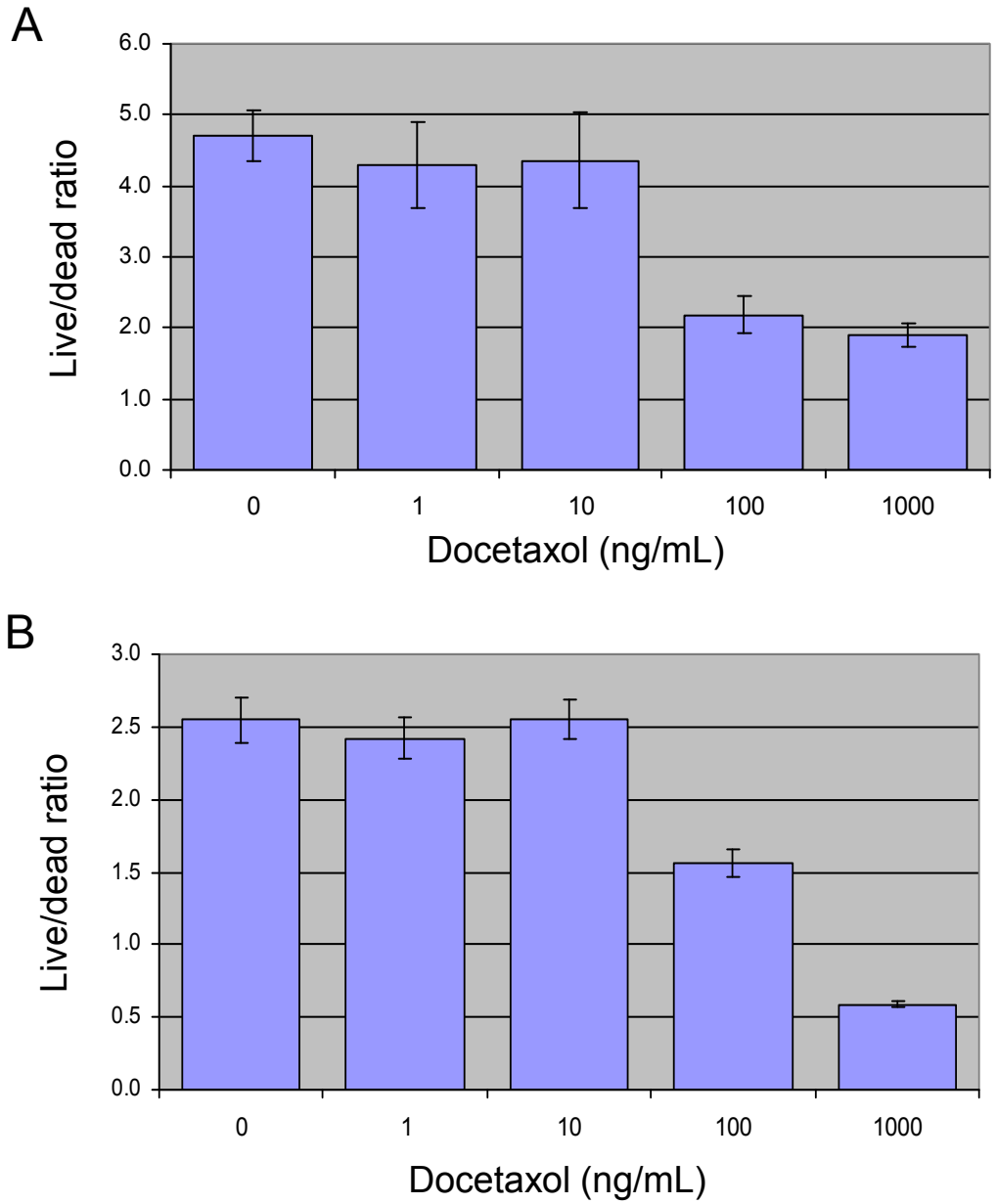

Supplemental Figure S7